Industrial Chemistry & Materials

ROYAL SOCIETY OF CHEMISTRY

MINI REVIEW

View Article Online
View Journal

Check for updates

Cite this: DOI: 10.1039/d5im00380f

Advanced photocatalysis enabled by water-state-driven interface design

Qian Zhang,†[a] Dongmin Liu,†[a] Bin Yang,[a] Hao Liu,[a] Guangfu Liao,*[b] Anna Lipovka,[d] Raul D. Rodriguez,*[d] Jun Li *[c] and Xin Jia *[a]

Photocatalytic conversion of abundant gaseous small molecules on Earth (such as CO_2, N_2, and O_2) into high-value chemicals is a promising strategy for renewable fuel production and environmental remediation. However, conventional gas–liquid photocatalytic interfaces face three unavoidable bottlenecks. Poor utilization of solar energy, rapid charge carrier recombination, and sluggish mass transfer limit the efficiencies of solar-to-fuel processes and the widespread application of photocatalysis in industry. Recent advances in water-state interface engineering, namely utilizing liquid, microdroplet, and vapor phases, have demonstrated unprecedented performance enhancements for earth-abundant gas conversions. This review critically analyzes mechanistic principles of phase-tailored photocatalyst design, elucidates interfacial charge and mass transfer dynamics, and discusses structure–activity relationships in CO_2 reduction, N_2 fixation, and H_2O_2 synthesis. Supported by recent experimental data, we highlight emerging opportunities in metastable interface engineering, offering actionable insights to overcome limitations in bi-phase systems. These innovations are critical for scalable solar chemical production, advancing the industrialization of photocatalytic technologies.

Received 19th December 2025,
Accepted 24th March 2026

DOI: 10.1039/d5im00380f

rsc.li/icm

Keywords: Photocatalysis; Phase interface; Liquid water; Microdroplets; Water vapor.

[a] School of Chemistry and Chemical Engineering, Shihezi University, Shihezi, 832003, P. R. China. E-mail: jiaxin@shzu.edu.cn
[b] National Forestry and Grassland Administration Key Laboratory of Plant Fiber Functional Materials, College of Materials Engineering, Fujian Agriculture and Forestry University, Fuzhou 350002, China. E-mail: liaogf@fafu.edu.cn
[c] Henan Institute of Advanced Technology, Zhengzhou University, Zhengzhou, 450052, P. R. China. E-mail: junli2019@zzu.edu.cn
[d] Tomsk Polytechnic University, 30 Lenin Avenue, 634050 Tomsk, Russia. E-mail: raul@tpu.ru
† These authors contributed equally to this work.

1 Introduction

The escalating global energy and environmental crisis, exacerbated by the unsustainable consumption of fossil fuels, have spurred an urgent demand for advanced sustainable energy conversion technologies. Emerging solutions, including solar photovoltaics, wind energy, electrocatalysis, hydropower, and carbon capture and utilization, hold significant promise for mitigating the detrimental impacts of

Qian Zhang

Qian Zhang received her bachelor's degree in Chemical Engineering and Technology in 2019 and her master's degree in Chemical Engineering in 2023. She is currently a doctoral candidate, majoring in Chemical Engineering and Technology at the School of Chemistry and Chemical Engineering, Shihezi University, China. Her main research interests focus on the structural control of catalytic materials and their application in the fields of energy and environment.

Dongmin Liu

Dongmin Liu received her bachelor's degree in Applied Chemistry in 2025. She is currently a master's student majoring in Materials and Chemical Engineering at the School of Chemistry and Chemical Engineering, Shihezi University, China. Her main research interest focuses on the structural control of photocatalytic materials and their application in agriculture.

Open Access Article. Published on 09 April 2026. Downloaded on 4/9/2026 9:59:55 PM.
This article is licensed under a Creative Commons Attribution-NonCommercial 3.0 Unported Licence.

© 2026 The Author(s). Co-published by the Institute of Process Engineering, Chinese Academy of Sciences and Royal Society of Chemistry

Open Access Article. Published on 09 April 2026. Downloaded on 4/9/2026 9:59:55 PM. This article is licensed under a Creative Commons Attribution-NonCommercial 3.0 Unported Licence.

fossil fuel dependence and facilitating the transition toward carbon neutrality goals.[1] Among these technologies, photocatalysis has emerged as a particularly promising approach due to its unique capability to directly utilize solar energy for the conversion of ubiquitous atmospheric small molecules (*e.g.*, H_2O, CO_2, N_2, O_2) into high-value chemicals, such as renewable fuels and fertilizers.[2,3]

Since the pioneering discovery of photocatalysis by Fujishima and Honda in 1972,[4] this environmentally friendly and cost-effective technology has demonstrated substantial potential for real-world implementation. A notable example is the work by Domen's group, who developed a 100 m^2 panel reactor based on aluminum-doped strontium titanate, achieving a solar-to-hydrogen (STH) efficiency of 0.76% with operational stability exceeding one year.[5] Inspired by natural photosynthesis, Li *et al.* introduced the concept of a "hydrogen farm" based on suspended photocatalyst nanoparticles for large-scale solar-driven water splitting. This system achieved a remarkable STH efficiency of over 1.8%, which is the highest reported value for overall water splitting to date.[6] Huang *et al.*, in turn, utilized the intrinsic polarization properties of polar crystals to induce enhanced internal electric fields, which promote photogenerated charge separation. This strategy allowed the use of these crystals as photocatalytic materials with enhanced performance.[7–9]

Despite their conceptual simplicity, conventional solid–liquid bi-phase photocatalytic systems, where chemical reactions occur at the interface between the solid photocatalyst and an aqueous medium, face significant challenges that limit their industrial applications. Three interrelated bottlenecks persist: (i) inefficient solar spectrum utilization due to limited light absorption, (ii) rapid recombination of photogenerated electron–hole pairs before interfacial charge transfer, and (iii) constrained mass transport of reactants to active sites. Despite significant advances in photocatalyst design and strong theoretical support, these inherent limitations continue to hinder the practical efficiency of biphasic systems below industrially viable thresholds.

Emerging phase-interface modulation strategies, achieved by controlling the states of water (namely, liquid water, microdroplets, and water vapor), can dramatically enhance photocatalytic performance by simultaneously addressing all three fundamental limitations. The development of innovative interfacial architectures, particularly gas–liquid–solid triphase and gas–solid biphasic systems, has enabled (i) broadband solar energy harvesting through enhanced light–matter interactions, (ii) efficient charge separation *via* interfacial electric fields or synergistic photothermal/hydrovoltaic effects, and (iii) optimal mass transport by circumventing traditional solubility and diffusion constraints for gaseous reactants. These tailored interfaces represent a paradigm shift in photocatalytic system design, offering new pathways to overcome the efficiency bottlenecks of conventional approaches.

The growing research interest in phase-interface engineering for photocatalysis is reflected in publication trends. The Web of Science search using keywords such as "three-phase photocatalysis", "gas–liquid–solid interface", "microdroplet photocatalysis", or "gas-phase photocatalysis" revealed over 1750 publications from 2015 to 2025, with approximately 1170 articles (67%) appearing in the most recent five-year period (2020–2025), as shown in Fig. 1. This trend highlights the swiftly growing interest and substantial advances in utilizing water-state modulation to design more efficient photocatalytic interfaces.

This review article aims to systematically analyze how phase-interface modulation, enabled by controlling water

Raul D. Rodriguez

Prof. Raul D. Rodriguez received his Ph.D. degree in Physics and Chemistry of Nanomaterials in 2009 with the highest honors from the Institut des NanoSciences de Paris, Pierre et Marie Curie University Paris, France. In 2011, he joined the DFG Research Unit Sensoric Micro- and Nano-Systems in the Semiconductor Physics group at TU Chemnitz, Germany. His experience includes implementing and developing novel methods for nanoscale characterization. He was appointed in 2017 as a Full Professor at Tomsk Polytechnic University. He focuses on flexible electronics, particularly novel plasmonic and 2D nanomaterials for technological developments, including biomedicine, optoelectronics, energy, and safety applications.

Xin Jia

Prof. Xin Jia obtained his Ph.D. degree from Lanzhou University, China in 2009. He began to work at Shihezi University in the same year and became a full professor in 2014. Now, he is Changjiang Distinguished Professor and Secretary of the Party Committee of the College of Chemistry and Chemical Engineering at Shihezi University. His research interests concentrate on the design and synthesis of functional polymers, material surface interface modification, and preparation and application of photocatalytic materials in agriculture. He has published more than 100 papers as the first author or corresponding author.

© 2026 The Author(s). Co-published by the Institute of Process Engineering, Chinese Academy of Sciences and Royal Society of Chemistry

Open Access Article. Published on 09 April 2026. Downloaded on 4/9/2026 9:59:55 PM.
This article is licensed under a Creative Commons Attribution-NonCommercial 3.0 Unported Licence.

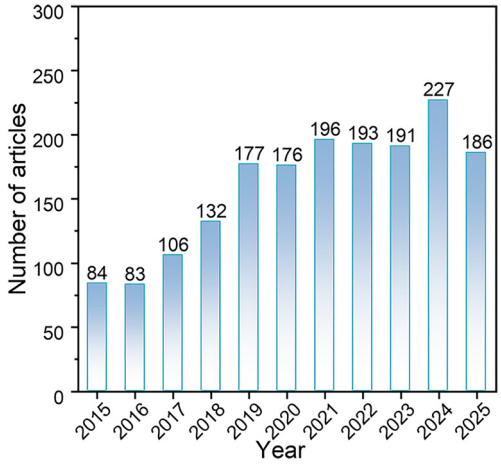

Fig. 1 Publication trends for phase-interface modulation in photocatalysis (2015–2025). Data retrieved from Web of Science.

states, enhances photocatalytic efficiency. The article is organized into four main sections:

Section 2 explains how three water states – liquid water, microdroplets, and water vapor – enhance photocatalytic efficiency. We explore the underlying mechanisms, highlight recent state-of-the-art developments, and identify current limitations and future directions for each approach.

Section 3 focuses on specific applications of the discussed phase-interface modulations in CO_2 reduction, H_2O_2 synthesis, and N_2 fixation. Through detailed examples and performance metrics, we evaluate the potential to overcome traditional limitations of photocatalysis.

In section 4, we summarize the key experimental and theoretical methods employed to unravel the structure–activity relationships and dynamic mechanisms at these advanced interfaces, providing a toolbox for future research in this field.

In section 5, we provide a summary and outlook highlighting the key advantages and practical implementations relevant to experts in materials science, photocatalysis, and energy conversion. We discuss open questions and research opportunities that could accelerate photocatalytic approaches toward industrial-scale sustainable energy and environmental solutions.

2 Phase-interface modulation *via* water state control

As stated in the introduction, conventional solid–liquid biphasic photocatalytic systems face fundamental challenges such as poor light utilization, rapid charge recombination, and inefficient mass transfer, which limit their practical application in industry. In this section, we systematically analyze three water-state-based interfacial systems, explaining how they enhance light harvesting, charge carrier dynamics, and reactant accessibility.

2.1 Liquid water

In conventional solid–liquid bi-phase photocatalytic systems, reactions occur at the interface between a solid photocatalyst and an aqueous medium. In contrast, gas–liquid–solid tri-phase interfaces in liquid water include gas as a third phase, positioning the photocatalyst at the water–gas boundary to allow direct sunlight exposure and access to gaseous reactants, thus overcoming the limitations of conventional systems. There is already solid evidence supporting the efficiency of such systems, as discussed in several studies.[10–18]

Mainly, such tri-phase interfaces are achieved through two configurations: (1) photocatalysts are immobilized on lightweight, hydrophobic carriers that float on water, or (2) modified photocatalysts with induced hydrophobicity are suspended in water. These interactions create a gas–liquid–solid interface that promotes photocatalytic reactions.

For case (1), photocatalysts like TiO_2 or g-C_3N_4 are loaded onto carriers such as carbon fiber, polystyrene,[19] melamine sponges,[15] polytetrafluoroethylene fiber films,[14,20,21] or hydrogels[12,18] *via* electrostatic assembly or *in situ* growth, allowing direct contact with gas reactants. In traditional solid–liquid two-phase systems, gaseous reactants (such as CO_2) need to dissolve in the aqueous phase before diffusing to the catalyst surface. Thus, this two-step process is fundamentally limited by the low solubility of gases in water (for CO_2-1.45 g L^{-1} at room temperature), resulting in limited mass transfer. In contrast, in the gas–liquid–solid three-phase system, the catalyst is deliberately positioned at the gas–water interface, enabling gaseous reactants to adsorb directly onto the catalyst surface from the gas phase, significantly increasing the local concentration of reactants and the mass transfer rate.[18,22]

For instance, Sheng *et al.* showed immobilizing TiO_2 on a superhydrophobic PTFE-treated carbon fiber substrate (Fig. 2a). This interface promoted a 10-fold increase (compared to a conventional system) in pollutant degradation rates under UV light by using O_2 as an electron scavenger to minimize electron–hole recombination and produce abundant reactive oxygen free radicals.[22] Similarly, Lee *et al.* reported a floatable elastomer–hydrogel nanocomposite photocatalytic platform, doubling H_2 production rates (163 mmol h^{-1} m^{-2}) compared to submerged systems by avoiding light attenuation and facilitating H_2 gas separation (Fig. 2b).[18]

In the second case, photocatalysts are modified with organic molecules like alkyl acids with different carbon chain lengths[23] or (3-aminopropyl) trimethoxysilane[24] by chemical bonding. This modification increases hydrophobicity and allows photocatalysts to suspend at the water–gas interface, enhancing O_2 adsorption and charge transfer. The three-phase systems mainly regulate the interface microenvironment by suppressing competitive side reactions (such as the hydrogen evolution reaction, HER)[10] and promoting the detachment of products. In traditional solid–liquid systems where the catalyst is fully immersed in

© 2026 The Author(s). Co-published by the Institute of Process Engineering, Chinese Academy of Sciences and Royal Society of Chemistry

Open Access Article. Published on 09 April 2026. Downloaded on 4/9/2026 9:59:55 PM.
This article is licensed under a Creative Commons Attribution-NonCommercial 3.0 Unported Licence.

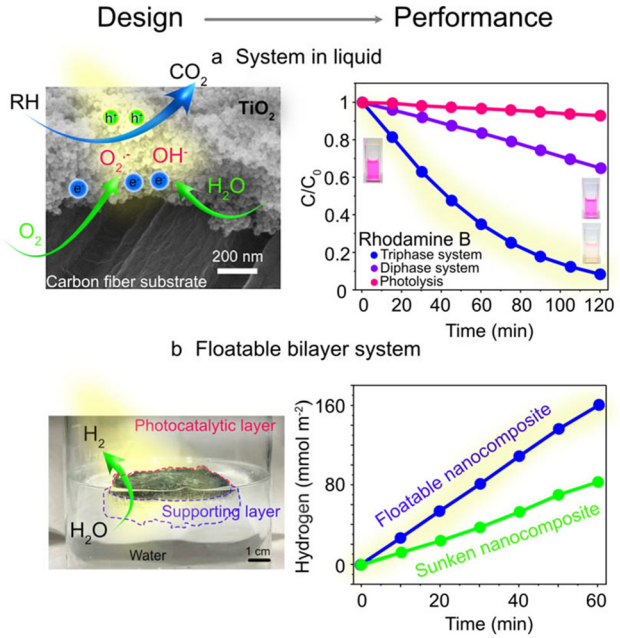

Fig. 2 Design and performance of photocatalytic platforms, exploiting gas–liquid–solid tri-phase interfaces in liquid water. (a) Scanning electron microscopy image of a tri-phase system together with the concept of photocatalytic reactions, implementation in rhodamine B degradation. Reprinted with permission from ref. 22. Copyright 2017, American Chemical Society; (b) floating nanocomposite promoting solar hydrogen production: photo, concept, and H_2 evolution rate. Reprinted with permission from ref. 18. Copyright 2023, Springer Nature.

water, the catalyst surface is saturated with water molecules, creating a high local proton concentration that favors the HER. In contrast, positioning the catalyst at the gas–water interface in a three-phase system spatially separates the catalyst from water, reducing the availability of protons at catalytic sites while maintaining direct access to gas. Additionally, at the gas–liquid–solid interface, the accessibility of the gas phase provides a thermodynamic driving force for volatile products (such as CO, CH_4, or H_2) to desorb rapidly into the gas phase rather than remaining adsorbed in the aqueous environment.[22,24]

Both approaches propose several advantages, including:

A. Enhanced solar light utilization because of the direct photocatalyst exposure to light;

B. Improved reactant accessibility caused by the facilitated adsorption and direct contact between the reactant and the photocatalyst;

C. Increased selectivity to the target product by suppressing side reactions and product decomposition;

D. Simplified recycling of the catalysts compared to solid–liquid systems.

The key consideration is how these tri-phase systems will function in real-world applications. Floating photocatalysts in the form of nets are ideal for *in situ* degradation of hydrophobic organic pollutants, such as polycyclic aromatic hydrocarbons, algal toxins, or pesticides. These photocatalytic nets do not sink, do not require mixing, and are easily recoverable.[25] Suspended photocatalysts, on the other hand, perform exceptionally well in continuous flow reactors. Such reactors can synthesize hydrogen peroxide *in situ* on a large scale for antibacterial and Fenton-like reactions, and can also produce liquid nitrogen fertilizer through nitrogen fixation to promote crop growth. Such systems take advantage of a large contact interface with dissolved pollutants and oxygen in the water.[26]

It is worth noting that these interfaces are relatively new, and challenges still exist in their implementation. For instance, the pending issues include weak binding between photocatalysts and hydrophobic carriers, which can lead to detachment during extended use; and difficulties in regulating hydrophilicity to optimize contact and photocatalytic activity. To address these issues, the current and future research should focus on developing robust carrier–photocatalyst interfaces and elucidating the relationship between hydrophobic microenvironments and photocatalytic performance to enable industrial-scale applications.

2.2 Microdroplets

Microdroplets are familiar to us as mist near waterfalls, clouds forming on mountains in the morning, or vapor from humidifiers. They are produced under the combined effects of surface tension and hydrodynamic forces, when liquid water breaks into tiny droplets (1–20 μm) under external forces like shear or electric fields, storing energy as surface tension. Unlike bulk water, microdroplets possess a high specific surface area, creating many gas–liquid interfaces with unique thermodynamic and kinetic properties that accelerate chemical reactions and enable interfacial catalysis.[27–29] These properties make microdroplets a promising platform for enhancing photocatalytic efficiency in gas–liquid–solid tri-phase systems. This section explores the surface electric fields of microdroplets and their coupling with photocatalysis, highlighting their mechanisms, applications in environmental pollutant management and clean energy production, and the challenges for industrial applications.

2.2.1 Surface electric field of microdroplets. It was shown experimentally and supported theoretically that the air–water interface of microdroplets generates extremely strong electric fields ($\sim 10^9$ V m^{-1}), acting as a new so-called "non-physical" catalyst to accelerate chemical reactions and control selectivity without external energy inputs.[30–32] Unlike externally applied electric fields (10^7–10^{10} V m^{-1}), which are challenging to generate and direct,[33,34] these spontaneous fields arise from charge separation at the droplet surface, enabling precise control of the reaction.[35–39]

For example, Xie *et al.* demonstrated that strong microdroplet electric fields reduce energy barriers in Menshutkin reactions, enhancing reaction rates.[40] This concept is shown in Fig. 3a. In another study, Wang *et al.*

© 2026 The Author(s). Co-published by the Institute of Process Engineering, Chinese Academy of Sciences and Royal Society of Chemistry

Open Access Article. Published on 09 April 2026. Downloaded on 4/9/2026 9:59:55 PM.
This article is licensed under a Creative Commons Attribution-NonCommercial 3.0 Unported Licence.

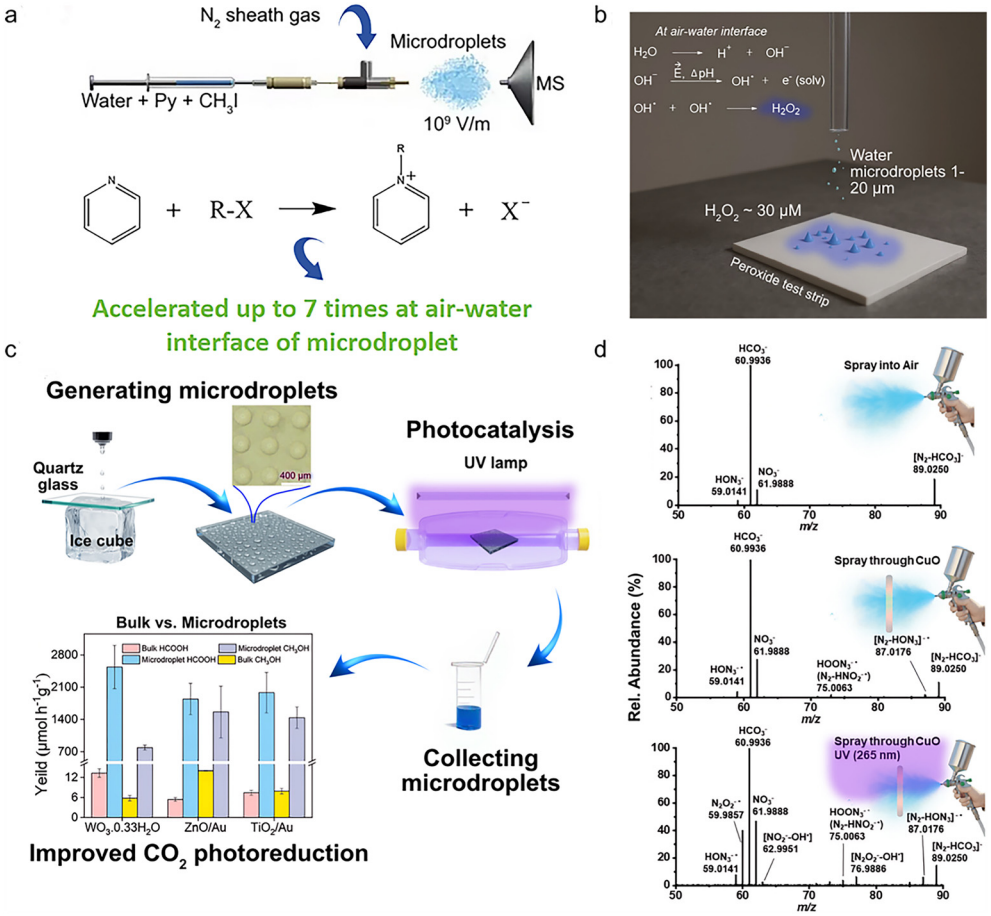

Fig. 3 Photocatalysis using microdroplets systems. (a) Reducing energy barriers in Menshutkin reactions. Reprinted with permission from ref. 40. Copyright 2023, American Chemical Society; (b) spontaneous production of H_2O_2 using microdroplets of pure water. Reprinted with permission from ref. 39. Copyright 2019, PNAS; (c) the most efficient CO_2 photoreduction using microdroplets: concept and performance. Reprinted with permission from ref. 52. Copyright 2023, Wiley-VCH GmbH; (d) real-time monitoring of the urea generation process by spraying water microdroplets and the $CuBi_2O_4$ catalyst. Reprinted with permission from ref. 54. Copyright 2023, American Chemical Society.

utilized Raman spectroscopy to study photochemical oxidation of organic matter with Fe(III)-oxalate in microdroplets, demonstrating that the surface electric field activates oxidants to generate free radicals and remove pollutants as visualized with rhodamine dye degradation.[41]

It has been reported that high electric fields within the microdroplets' surface can catalyze chemical reactions and break water molecules, leading to the production of strongly reducing free electrons and hydroxyl radicals.[42–45] In 2019, Zare *et al.* revealed for the first time that microdroplets of pure water spontaneously produce hydrogen peroxide (H_2O_2) at their surfaces.[39] This concept is illustrated in Fig. 3b where the proposed mechanism involves ·OH recombination at the interface, which are generated by the loss of electrons from OH^- at the surface of the water microdroplets.

These electric field-driven properties make microdroplets a versatile platform for accelerating reaction rates in applications like organic synthesis, pollutant degradation and H_2O_2 synthesis. However, these reactions currently suffer from low efficiency due to limitations in scalability and droplet stability control. Therefore, it is essential to integrate these methods with other technologies.

2.2.2 Enhancing the efficiency of photocatalysis with microdroplets. There are many ways to enhance the efficiency of photocatalysis by coupling it with other technologies.[46–48] One promising approach involves applying an external electric field.[49] This section discusses the use of microdroplets to create gas–liquid–solid tri-phase interfaces leveraging the droplet's strong interfacial electric fields and high surface area to enhance photocatalytic efficiency.

For example, Zare *et al.* significantly enhanced the stereoselective reduction of ketones to chiral alcohols by using enzymes, photosensitizers, cofactors, and triethanolamine in microdroplet form. Switching to microdroplets from the bulk state contributed to reducing the optical path of transmitted light, resulting in increased light intensity that promoted photocatalysis, reaching yields 1.5–5.6 times higher than in bi-phase systems.[50]

Using microdroplets indeed can significantly boost photocatalysis because of several configuration advantages:[51,52]

© 2026 The Author(s). Co-published by the Institute of Process Engineering, Chinese Academy of Sciences and Royal Society of Chemistry

Open Access Article. Published on 09 April 2026. Downloaded on 4/9/2026 9:59:55 PM.
This article is licensed under a Creative Commons Attribution-NonCommercial 3.0 Unported Licence.

A. The strong gas–liquid interfacial electric field within microdroplets generates a powerful driving force for the separation of photogenerated charge carriers.

B. Microdroplets improve the adsorption of gaseous reactants, promoting their enrichment at the interface, and enabling more efficient interactions and mass transfer.

C. The unique shape and refractive properties of microdroplets enhance local light absorption, thus improving the photocatalytic activity.

D. Additionally, the unique phase interface of microdroplets can lower the reaction energy barrier and improve selectivity.

The aforementioned advantages, particularly the enhanced adsorption of gaseous reactants (B), stem from the multiple effects of the droplet system: firstly, the extremely high specific surface area provides sufficient contact interfaces; secondly, the strong self-generated electric field at the interface ($\sim 10^9$ V m^{-1}) can polarize the reactant molecules, promoting their enrichment and activation through electrostatic interactions; thirdly, the thermodynamic surface enrichment effect caused by the curved interface further enhances the local concentration of reactants in the interface region; finally, the droplets' micrometer-scale size reduces the gas transport resistance significantly. The synergy of these effects collectively surpasses traditional bulk or conventional two-phase systems, achieving a significant enhancement in the adsorption and transport of gaseous reactants.[27–32,35–38]

Technically, there are two ways to couple microdroplets with photocatalysis:

(1) Dispersing photocatalyst powder in liquid water and generating microdroplets of the suspension using a microdroplet generator to enhance the contact area between the photocatalyst and the reactants, improving reaction efficiency[51,52] (see Fig. 3c).

(2) Spraying microdroplets of water directly onto a surface coated with the photocatalyst for the reaction to occur.[53] For instance, this approach was used for urea synthesis[54] (see Fig. 3d).

Both methods are viable, each with its pros and cons, and the choice depends on the specific requirements of the application. For instance, spraying water microdroplets (2) makes the recycling and reuse of the photocatalysts easier. However, as the reaction proceeds, the hydrophilic surface of the catalyst tends to become saturated with water, potentially hindering effective interaction with fresh microdroplets and reducing efficiency.

The proposed tri-phase interfaces in microdroplets could be adapted to several practical applications. For instance, in industrial exhaust gas treatment, particularly from petrochemicals, printing, painting, and semiconductor fabrication, microdroplets can capture volatile organic compounds (VOCs). These VOCs accumulate at the droplet surface, where loaded photocatalysts generate reactive radicals under UV illumination, leading to the mineralization of VOCs into CO_2 and H_2O.[55] Another demonstrated industrial application is high-value chemical synthesis. Microdroplet reactors act as continuous flow platforms, dispersing reactants and photocatalysts to accelerate light-driven reactions like oxidation, C–H activation, asymmetric synthesis, hydrogenation, and dehydrogenation.[56–58] Lastly, these interfaces play a crucial role in photocatalytic CO_2 utilization, H_2O_2 production and N_2 fixation. Microdroplets enhance these photocatalytic reactions by improving gas solubility and reaction kinetics, supporting sustainable fuel production.

In recent years, microdroplet-based interfaces have shown remarkable potential for enhancing photocatalytic efficiency. However, these systems remain relatively rare, which results in limited exploration of the full range of photocatalytic reactions and materials compatible with microdroplet environments. To unlock their full potential in energy and environmental applications, we believe that future research should prioritize the development of stable photocatalyst-microdroplet systems, the investigation of new reaction types, and the improved design of scalable microdroplet reactors.

2.3 Water vapor

A further reduction of microdroplets in size leads to another water state useful for photocatalysis: water vapor. This medium is environmentally friendly and sustainable, offering several advantages in heterogeneous catalytic systems. It's low viscosity, high polarity, and dynamic adsorption properties can enhance dynamic interactions between gaseous reactants and the photocatalyst's active sites.[59] This section explores the effects and mechanisms of water vapor systems in clean energy production and environmental remediation, including applications in water decomposition, CO_2 or N_2 reduction, and challenges associated with practical implementation.

Water vapor is used in solid–gas bi-phase interfaces to significantly enhance photocatalytic activity. For instance, Suguro *et al.* demonstrated efficient overall water splitting using Al-doped $SrTiO_3$ photocatalysts coated with TiO_x or TaO_x nanomembranes under vapor feeding. The system maintained a STH efficiency of 0.4% over 100 hours, even with using seawater as the vapor source. This approach minimizes the reverse O_2 reduction to H_2O, a common issue in solid–liquid systems.[60]

There are two primary approaches for achieving water vapor-based interfaces. The first approach involves directly introducing water vapor into the reactor. Zhang *et al.* used this approach to tackle the issue of O_2 reverse reduction to H_2O and developed three COF-based photocatalysts which are denoted as Pt@Tp-TAPB-COF (Tp = 1,3,5-triformylphloroglucinol, TAPB = 1,3,5-tris(4-aminophenyl)benzene), Pt@Tp-TAPT-COF (TAPT = 2,4,6-tris(4-aminophenyl)-1,3,5-triazine), and Pt@Tp-TAPyT-COF (TAPyT = tripyridyltriazine).

Among them, Pt@Tp-TAPyT-COF exhibits the best photocatalytic overall water splitting activity (Fig. 4a). The core reason behind this superior performance originates

© 2026 The Author(s). Co-published by the Institute of Process Engineering, Chinese Academy of Sciences and Royal Society of Chemistry

Open Access Article. Published on 09 April 2026. Downloaded on 4/9/2026 9:59:55 PM.
This article is licensed under a Creative Commons Attribution-NonCommercial 3.0 Unported Licence.

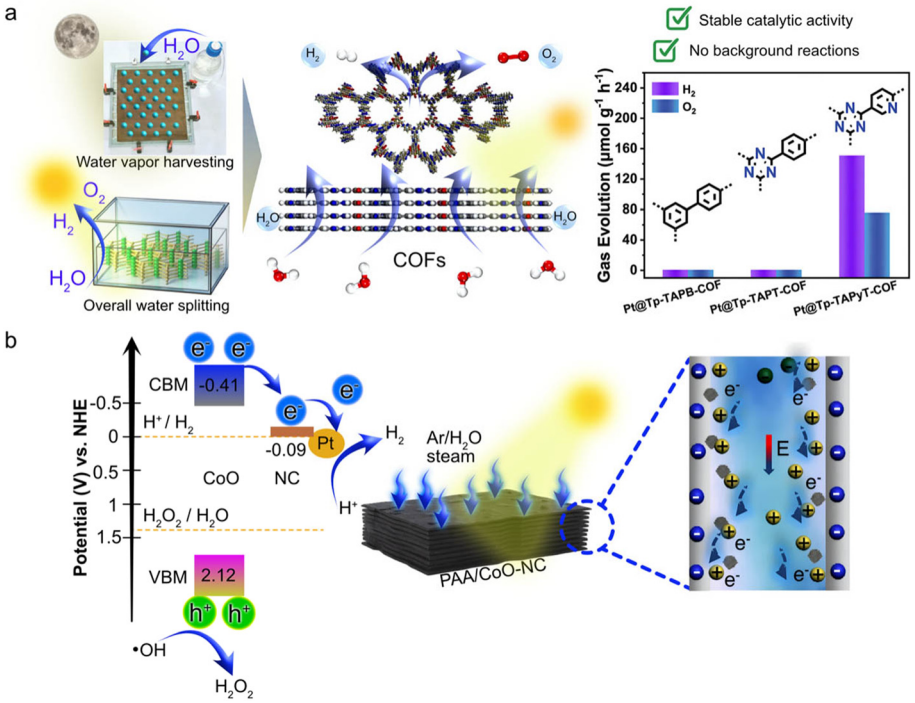

Fig. 4 Water vapor systems in photocatalysis. (a) Schematic diagram of COF photocatalysts for overall water vapor splitting and gas evolution metrics. Reprinted with permission from ref. 61. Copyright 2025, Wiley-VCH GmbH; (b) the band structure and schematic illustration of hydrovoltaic effect-enhanced photocatalytic water splitting. Reprinted with permission from ref. 65. Copyright 2023, Springer Nature.

from several synergistic reasons. First of all, the unique composite structure provides abundant active sites; second, the *in situ* deposited Pt nanoparticles function both as active sites for the HER and as electron-withdrawing centers that create strong electronic coupling with the COF framework, facilitating efficient charge separation; third, the pyridine-N atoms in the catalyst skeleton reduce the Gibbs free energy barrier of the OER, accelerating O_2 generation and promoting its rapid desorption before photogenerated electrons can reduce it back to water. Unlike a traditional solid–liquid reaction system, the catalyst in the gas–solid reaction system has no direct contact with liquid water. This spatial separation prevents dissolved O_2 from accumulating photogenerated electrons on the catalyst, fundamentally suppressing the competing O_2 reduction pathway and enabling efficient overall water splitting.[61]

Notably, the gas–solid bi-phase interfaces formed between water vapor and the photocatalyst could also exhibit photothermal or hydrovoltaic effects. These effects optimize charge carrier separation and proton migration, thus enhancing solar energy conversion efficiency. The second approach involves loading photocatalysts with photothermal materials to generate water vapor *in situ* through photothermal water evaporation. This photothermal effect enhances reaction efficiency by converting sunlight, especially in the visible and near-infrared range, into thermal energy, which facilitates water vapor generation and accelerates different photocatalytic processes. In addition, the heat generated by the photothermal base can be radiated to accelerate carrier separation and the desorption of gaseous products, further promoting the photocatalytic reaction.

In this context, Li *et al.* developed a photothermal/photocatalytic Z-scheme heterojunction by combining $ZnIn_2S_4$-WO_3 with carbonized wood (C-wood), achieving a STH efficiency of 1.52% for overall water splitting. The C-wood serves as a bridge to enhance charge carrier separation and facilitate the transfer of photogenerated carriers, making this photothermal approach promising for increasing efficiency.[62] Additionally, the photothermal effect allows for simultaneous freshwater collection, as demonstrated by Bu *et al.* with a biomimetic COF aerogel photocatalyst that produces H_2O_2 while desalinating water.[63]

Besides the photothermal effect, the photovoltaic effect also plays a significant role. The hydrovoltaic effect refers to the direct conversion of kinetic energy from water molecules into electrical energy through interactions between functional materials and water.[64] In photocatalysis, this effect occurs at gas–solid interfaces, generating a potential gradient from interfacial water flow (*e.g.*, evaporation, capillarity, or ionic diffusion), which forms a built-in electric field that promotes the directional separation of photogenerated electrons and holes.

For instance, Xin *et al.* developed a PAA/CoO-NC photocatalyst by combining poly(acrylic acid) with cobalt oxide-modified nitrogen-doped carbon (NC) to simultaneously produce H_2 and H_2O_2 *via* photocatalytic water splitting[65] (Fig. 4b). The generation of hydrovoltaic potential in the PAA/CoO-NC system is mainly attributed to the

© 2026 The Author(s). Co-published by the Institute of Process Engineering, Chinese Academy of Sciences and Royal Society of Chemistry

Open Access Article. Published on 09 April 2026. Downloaded on 4/9/2026 9:59:55 PM.
This article is licensed under a Creative Commons Attribution-NonCommercial 3.0 Unported Licence.

directional migration and charge separation of H^+ induced by water vapor diffusion. This hydrovoltaic effect strengthens interactions between protons and reaction centers of photocatalysts, improving electron transport and water splitting efficiency. The catalyst design involves several key benefits: (1) the high density of carboxylic groups in PAA renders the composite surface negatively charged, facilitating H^+ enrichment and directional migration; (2) the porous structure enables continuous vapor flux, maintains the contact between the hydrovoltaic PAA and photocatalytic CoO-NC components, and sustains the humidity gradient required for H^+ migration; (3) the hydrovoltaic effect reduces the Schottky barrier at the CoO-NC interface by 33%, significantly promoting charge separation. This combined mechanism of water vapor generating electrostatic potential (hydrovoltaic effect) while light generates photovoltaic potential is the reason for the superior water splitting efficiency of this system. The hydrovoltaic effect, driven by H^+ diffusion, strengthens interactions between protons and reaction centers of photocatalysts, improving electron transport and water splitting efficiency. Similarly, Yang *et al.* integrated photocatalytic H_2 evolution with the hydrovoltaic effect in a water generator, reconfiguring ion gradients for continuous current output, thereby enhancing hydrovaporation performance.[64]

The number of research reports using the hydrovoltaic effect in photocatalysis is limited, with only a few studies reported on this. To advance practical applications in clean energy and environmental remediation, future research should focus on developing materials that exhibit a strong hydrovoltaic effect as well as on investigating interfacial dynamics of water molecules to enhance photocatalytic efficiency.

Despite these advantages, several challenges remain. For example, water molecules have strong polarity and hydrogen bonding ability, which leads to competitive adsorption at active sites, hindering reactant (*e.g.*, organic pollutant molecules, CO_2, O_2) access as well as product desorption. Additionally, high water vapor concentrations can compete for photogenerated charges during gaseous reactants, promoting unwanted side reactions. In the future, in response to the aforementioned challenges, we should focus on designing specific photocatalysts and reactors to optimize the interface between water vapor, catalysts and gaseous reactants, thereby enhancing the photocatalytic efficiency.

2.4 Summary

Section 2 has systematically elucidated the "water-state-driven" paradigm for interface design in photocatalysis. The core idea behind this concept is that water acts not merely as a solvent or reactant, but its physical state can be leveraged as a primary driver for optimized reaction microenvironments. Specifically:

Liquid water drives the creation of gas–liquid–solid triphase interfaces through buoyancy and tailored wettability. This design directly addresses the limitations of gas solubility and light penetration by positioning the catalyst at the water–gas boundary.

Microdroplets drive the formation of high-curvature gas–liquid interfaces characterized by an immense specific surface area and a spontaneously generated intense electric field. These properties concurrently facilitate enhanced local reactant concentration and dramatically accelerated charge separation.

Water vapor drives the establishment of dynamic gas–solid biphasic interfaces. Its low viscosity results in rapid mass transfer, while its interaction with functional materials can induce synergistic photothermal or hydrovoltaic effects, further promoting efficient proton transfer and product desorption.

In each case, the transition from a passive aqueous medium to an actively engineered water-state-based interface provides a targeted solution to the fundamental bottlenecks plaguing conventional photocatalysis.

3 Photocatalytic applications

The modulation of phase interfaces *via* water state control has been widely applied to enhance the photocatalytic conversion of Earth's abundant small molecules into valuable chemicals. This approach demonstrates superior catalytic activity and selectivity compared to conventional solid–liquid bi-phase interfaces in reactions such as CO_2 reduction, H_2O_2 production, and N_2 fixation.[22,66,67] In this section, we summarize the progress in phase-interface modulation for these three reactions utilizing liquid water, microdroplets, and water vapor. We highlight the advantages of phase-interface modulation, the rationality behind catalyst design, the underlying mechanisms, and compare catalytic performance.

3.1 Photocatalytic CO_2 reduction

The excessive greenhouse gas emissions, primarily CO_2, due to the overconsumption of fossil fuels, have raised significant concerns. The photocatalytic CO_2 reduction reaction (CO_2RR) offers a sustainable solution by converting CO_2 into valuable carbon derivatives, such as CO, CH_4, CH_3OH, and C_2H_4. These reactions are particularly interesting for researchers and engineers because they can occur under mild conditions.

Over the past decade, efforts have largely focused on designing photocatalysts for conventional bi-phase interfaces to enhance the efficiency of CO_2RR. However, the low solubility and diffusion of CO_2 in water at these interfaces significantly hinder photocatalytic efficiency. This subsection discusses successful examples of three different interfaces that have been developed to improve CO_2RR. To highlight the advantages of the novel interfaces, we also summarized the CO_2RR activity under a water-state-driven interface in Table 1.

3.1.1 Photocatalytic CO_2RR in liquid water. An additional liquid water phase ensures the improved CO_2 supply for

© 2026 The Author(s). Co-published by the Institute of Process Engineering, Chinese Academy of Sciences and Royal Society of Chemistry

Open Access Article. Published on 09 April 2026. Downloaded on 4/9/2026 9:59:55 PM.
This article is licensed under a Creative Commons Attribution-NonCommercial 3.0 Unported Licence.

Table 1 Summary of the photocatalytic CO_2RR activity under a water-state-driven interface

Water state	Material design	Light source	Reaction conditions	Product rate (μmol g^{-1} h^{-1})	Selectivity for CO_2RR	Enhancement factor	Ref.
Liquid water	Ag–TiO_2-GDL	300 W Xe lamp ($\lambda \leq 400$ nm)	Three-phase interface; catalyst floated onto the surface of the water	CO: 220 CH_4: 100	97.8%	8 times	68
	NAL-MRF	Not available	Three-phase interface; hydrophobic catalyst suspended in water	CH_3OH: 31.41	93.62%	4.2 times	75
	Pt/*o*-PCN	Visible-light irradiation	Three-phase interface; hydrophobic catalyst suspended in water	CO: 286 CH_4: 136	87.9%	34 times	69
	Cu_2O–Ag–TiO_2/PTFE	Two-sided illumination was implemented from both the top and bottom with uniform light intensities	Three-phase interface; catalyst floated onto the surface of the water	CO: 347.4 CH_4: 25.1	96.2%	120 times	14
	g-C_3N_4/$CuFe_2O_4$/$ZnIn_2S_4$	Visible-light irradiation	Three-phase interface; catalyst suspended in water	CH_4: 267.4	96.8%	2 times	76
	Try-CD/CN	300 W Xe lamp ($\lambda \geq 420$ nm)	Three-phase interface; hydrophobic catalyst suspended in water	CH_4: 17.1	97%	6.7 times	10
Microdroplets	$WO_3 \cdot 0.33H_2O$	365 nm UV lamp	Gas–liquid interface; catalysts presented in microdroplets	HCOOH: 2536	Not available	195 times	52
Water vapour	CD/V_OR-BMO-1.2	Not available	The catalyst is in an atmosphere of water vapor and CO_2	CO: 60	100%	Not available	72
	CeO_2	300 W Xe lamp (AM 1.5 G)	The catalyst is in an atmosphere of water vapor and CO_2	CH_4: 192.75	100%	Not available	73
	TiO_2/$SrTiO_3$	300 W Xe lamp (100 mW cm^{-2})	The catalyst is in an atmosphere of water vapor and CO_2	CO: 100 CH_4: 47	100%	Not available	70

photocatalytic CO_2RR. To address the challenge of low CO_2 solubility and diffusion in water, Zhang *et al.* designed a tri-phase system with Ag-decorated TiO_2 nanoparticles at the gas–water boundary. This configuration, characterized by a hydrophobic–hydrophilic transition, promotes the mass transfer of gaseous CO_2 and liquid water molecules at the interface, as illustrated in Fig. 5a. The presented system was deliberately engineered to ensure a wettability gradient between the catalyst support (such as hydrophobic carbon paper or PTFE membrane) and the loaded nanocatalyst (such as hydrophilic Ag–TiO_2). Such a contrast in wetting properties performs two functions. The hydrophobic substrate repels bulk water, creating open gas channels that allow unobstructed CO_2 transport from the gas phase directly to the catalyst surface, while the hydrophilic Ag–TiO_2 efficiently captures protons, maintaining a hydrated environment. This design results in the precisely controlled three-phase (gas–liquid–solid) contact line, being distinctly different from many gas diffusion electrodes (GDEs) or membrane electrode assemblies (MEAs), which typically employ uniformly hydrophobic porous structures to ensure gas permeability throughout the entire electrode thickness. This design achieves a CO_2RR rate exceeding 300 μmol g^{-1} h^{-1}, with a selectivity of 97.8% for carbon-containing products.[68]

The theoretical potential of photocatalytic CO_2RR is comparable to that of the hydrogen evolution reaction (HER), making the HER the primary competing process affecting CO_2RR selectivity and efficiency. While protons (H^+) are abundant in aqueous solutions because of water ionization, CO_2 availability at the photocatalyst surface is limited by its low solubility and slow diffusion. Therefore, enhancing CO_2 accessibility while reducing proton concentration is critical to suppressing the HER. Recent studies demonstrate that solid–liquid–gas tri-phase interfaces in liquid water effectively mitigate the HER and enhance CO_2RR. For example, Antonietti *et al.* developed a hydrophobic photocatalyst surface that facilitates direct contact between gas-phase CO_2, liquid water, and the solid catalyst. This design successfully

© 2026 The Author(s). Co-published by the Institute of Process Engineering, Chinese Academy of Sciences and Royal Society of Chemistry

Open Access Article. Published on 09 April 2026. Downloaded on 4/9/2026 9:59:55 PM.
This article is licensed under a Creative Commons Attribution-NonCommercial 3.0 Unported Licence.

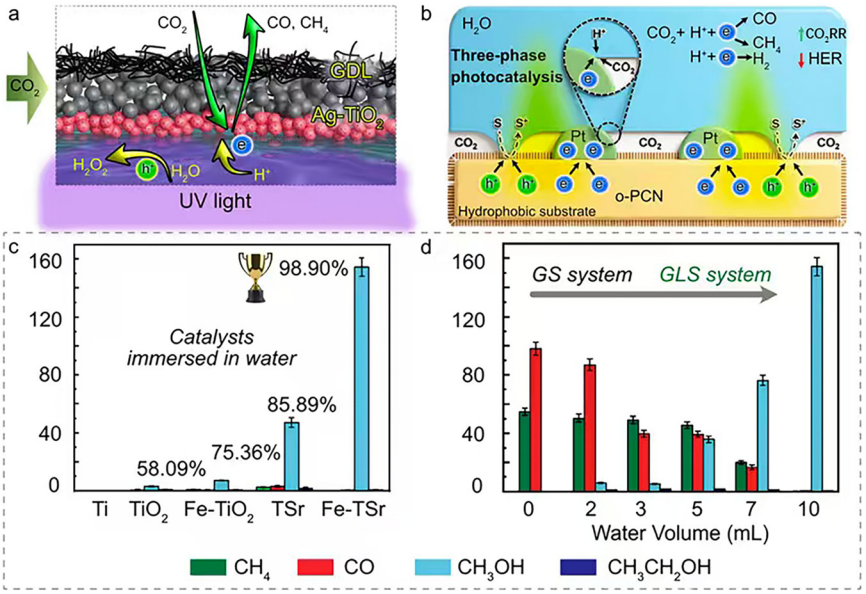

Fig. 5 (a) Schematic illustration of the triphase photocatalytic CO_2RR system based on Ag-TiO_2. Reprinted with permission from ref. 68. Copyright 2022, Wiley-VCH GmbH; (b) scheme of the three-phase photocatalyst Pt/*o*-PCN and the mechanism of three-phase photocatalysis. Reprinted with permission from ref. 69. Copyright 2019, Wiley-VCH GmbH; (c) CO_2 photoreduction for 5 h on different samples in 10 mL pure water; (d) CO_2 photoreduction on Fe-TSr with different volumes of water. Reprinted with permission from ref. 70. Copyright 2023, Wiley-VCH GmbH.

overcomes CO_2 mass transfer limitations, maintaining an impressive 87.9% selectivity for CO_2RR, even when using a platinum co-catalyst, a well-known HER-favoring material, as shown in Fig. 5b.[69]

A typical CO_2RR involves both CO_2 reduction and water oxidation, which require different environments: gas–solid for CO_2 reduction and solid–liquid for water oxidation. To overcome this challenge, Xie *et al.* designed a photocatalyst by subsequently depositing Cu_2O, Ag, and TiO_2 layers on a floatable polytetrafluoroethylene (PTFE) membrane. While the system floats on water under illumination, it enables two simultaneous processes: 1) photogenerated electrons get transferred to the gas-exposed Cu_2O side for CO_2 reduction, and 2) holes are directed to the water-immersed TiO_2 side for water oxidation. This innovative configuration leads to high selectivity for CO_2RR and H_2O_2 production while suppressing the HER.[14,70]

Conventional photocatalytic CO_2RR faces several challenges, including limited CO_2 accessibility and competition with the HER, which have been effectively addressed in previous studies, as cited above. However, a significant issue is poor product selectivity, partially attributed to interfacial wettability. Hydrophilic surfaces easily bind water molecules and favor the HER, while hydrophobic surfaces enhance CO_2 adsorption and promote CO_2RR. This means that the distribution of intermediates and the reaction mechanism can be changed by altering the wettability. Huang *et al.* experimentally indicated this by modifying C_3N_4 with hydrophobic carbonaceous co-catalysts (Try-CDs), constructing a tri-phase interface between CO_2, the catalyst, and water. This Try-CD/C_3N_4 design allowed 97% selectivity for CH_4 with a yield of 17.1 μmol g^{-1} h^{-1}, which is 6.7 times higher than that of pristine C_3N_4.[10]

3.1.2 Photocatalytic CO_2RR in microdroplets. Microdroplet systems enhance CO_2RR due to their unique gas–liquid interfacial properties, offering two advantages. First, as was discussed above, the strong electric field at the microdroplet interface drives efficient separation of photogenerated electron–hole pairs, and second, this interfacial effect can significantly enhance the adsorption capacity and local concentration of CO_2 molecules. The high potential of microdroplets in CO_2RR was summarized in a recent review article by Y. Zhang.[71] In this context we must mention again the work of Zhang's team[52] (Fig. 3c). Their innovation is in designing a photocatalytically coupled microdroplet system based on WO_3-0.33H_2O as the photocatalyst, which allowed achievement of a formic acid production rate of 2536 μmol h^{-1} g^{-1} without the need for sacrificial agents. This is a remarkable 200-fold improvement over conventional solid–liquid bi-phase interfaces (13 μmol h^{-1} g^{-1}). The superior performance of WO_3-0.33H_2O is not attributable to a single factor alone, but rather to the synergistic effect of its high electrical conductivity, suitable band structure, and nanotube morphology. Assisted by the strong interfacial electric field of the microdroplet system, these advantages are further amplified, resulting in a far superior yield compared to the other two catalysts. To show that the carbon atoms in the generated formic acid are entirely derived from $^{13}CO_2$, the authors conducted a rigorous ^{13}C isotope labeling experiment, thereby ruling out the possibility that the catalyst itself or the oxidation

© 2026 The Author(s). Co-published by the Institute of Process Engineering, Chinese Academy of Sciences and Royal Society of Chemistry

Open Access Article. Published on 09 April 2026. Downloaded on 4/9/2026 9:59:55 PM.
This article is licensed under a Creative Commons Attribution-NonCommercial 3.0 Unported Licence.

of organic substances could serve as the carbon source. Of particularly high practical relevance, the team demonstrated the scalability of their system by generating large quantities of microdroplets using an electrosprayer, offering valuable insights for future large-scale photocatalytic CO_2RR applications.

3.1.3 Photocatalytic CO_2RR in water vapor. The gas–solid biphasic interface in water vapor is promising to overcome the limitations of limited CO_2 solubility in solvents, weak CO_2 adsorption, and difficulties in separating liquid products, typically existing in conventional CO_2RR.[72–74] In such systems, photocatalyst particles are uniformly distributed on a substrate, allowing direct contact with a mixture of CO_2 and H_2O. The CO_2 concentration can be freely adjusted, while a minimal amount of H_2O provides protons, typically suppressing the unwanted HER due to the CO_2-rich atmosphere.

In this context, Huang *et al.* developed a Fe@TiO_2/$SrTiO_3$ heterostructured nanotube array photocatalyst with excellent CO_2RR activity and stability.[70] By regulating the water state, the researchers achieved selective synthesis: submerged catalysts in liquid water led to selective CO_2RR to prepare CH_3OH with over 98.9% selectivity, while CO_2RR under water vapor yielded syngas (CO/CH_4) with over 99.9% selectivity. The mechanism revealed that in liquid water, abundant ·OH radicals and H_2O molecules around monatomic Fe inhibit the dehydration reaction (1), favoring CH_3OH formation.

$$\cdot COH + H^+ + e^- \rightarrow \cdot C + H_2O \quad (1)$$

In contrast, reduced ·OH and H_2O levels in water vapor facilitate this dehydration, leading to the production of ·CH, ·CH_2, ·CH_3, and CH_4. This study provides a valuable reference for controlling water states to achieve selective regulation of photocatalytic CO_2RR.

3.2 Photocatalytic H_2O_2 synthesis

H_2O_2 is a green chemical, playing a vital role in energy, environmental applications, and chemical synthesis. However, the growing market demands, as well as the limitations of conventional anthraquinone technology have contributed to the need for sustainable H_2O_2 synthesis approaches. Photocatalysis is indeed a promising eco-friendly strategy, which utilizes only sunlight, H_2O and O_2 to produce H_2O_2.

For the purpose of H_2O_2 synthesis, conventional solid–liquid bi-phase interfaces involve immersing powdered photocatalysts in water. The whole process mainly takes place *via* two possible pathways:

(1) Two-step O_2 reduction, following reactions (2) and (3):

$$O_2 + e^- \rightarrow \cdot O_{2^-} \quad (2)$$

$$\cdot O_{2^-} + e^- + 2H^+ \rightarrow H_2O_2 \quad (3)$$

(2) Direct one-step two-electron O_2 reduction, following reaction (4):

$$O_2 + 2e^- + 2H^+ \rightarrow H_2O_2 \quad (4)$$

Table 2 Summary of the photocatalytic H_2O_2 activity under a water-state-driven interface

Water state	Material design	Light source	Reaction conditions	Product rate (μmol g^{-1} h^{-1})	Apparent quantum efficiency (%)	Enhancement factor	Ref.
Liquid water	2 L-mCN/F-Naf	300 W Xe lamp ($\lambda \leq 400$ nm)	Three-phase interface; catalyst floated onto the surface of the aqueous ethanol solution	5380	2.1 at 400 nm	Not available	21
	M-SBP	100 W LED lamp ($\lambda \geq 420$ nm)	Three-phase interface; catalyst floated onto the surface of the water	717.5	2.9 at 420 nm	3.3 times	77
	TPB-DMTP-COF	300 W Xe lamp ($\lambda \geq 420$ nm)	Three-phase interface; catalyst floated onto the surface of the water	2882	18.4 at 420 nm	15 times	16
	TiO_2/Pt/Co POM	5 W lamp ($\lambda = 365$ nm)	Three-phase interface; catalyst floated onto the surface of the aqueous methanol solution	1395	1.09 at 420 nm	5 times	79
	CTTP	300 W Xe lamp (AM1.5G filter)	Three-phase interface; catalyst floated onto the surface of the water	1858	1.08 at 420 nm	14 times	13
	Cv-PCN	300 W Xe lamp (AM1.5G filter)	Three-phase interface; catalyst floated onto the surface of the water	2063	26.8 at 400 nm	10 times	17
	Pd/A/$BiVO_4$	300 W Xe lamp ($\lambda \geq 420$ nm)	Three-phase interface; catalyst suspended in water	805.9	6.02 at 400 nm	Not available	24
	TBO40	300 W Xe lamp ($780 \geq \lambda \geq 350$ nm)	Three-phase interface; catalyst floated onto the surface of furfuryl alcohol aqueous solution	57 500	1.25 at 365 nm	6 times	19
Microdroplets	g-C_3N_4	365 nm UV lamp (2.32 mW cm^{-2})	Gas–liquid interface; catalysts presented in microdroplets with Triethanolamine	20 600	Not available	75 times	51

© 2026 The Author(s). Co-published by the Institute of Process Engineering, Chinese Academy of Sciences and Royal Society of Chemistry

Open Access Article. Published on 09 April 2026. Downloaded on 4/9/2026 9:59:55 PM.
This article is licensed under a Creative Commons Attribution-NonCommercial 3.0 Unported Licence.

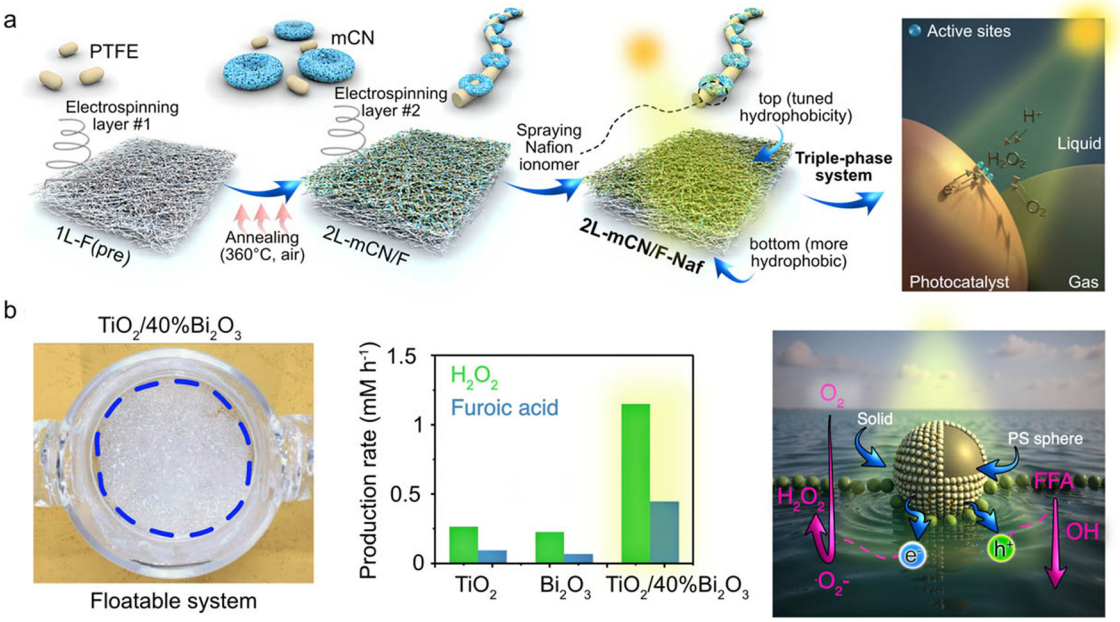

Fig. 6 (a) Schematic illustration of the synthesis route for the Janus 2 L-mCN/F-Naf fiber membrane and photocatalytic O_2 reduction to H_2O_2. Reprinted with permission from ref. 21. Copyright 2024, American Chemical Society; (b) floatable S-scheme TiO_2/Bi_2O_3 photocatalyst, production rates of H_2O_2 and FA for 12 hours, schematic illustration of the photoredox reaction in the proposed system. Reprinted with permission from ref. 19. Copyright 2022, Wiley-VCH GmbH.

However, the efficiency of H_2O_2 synthesis is limited by low solubility (0.9 mM, 298 K, 1 atm) and slow diffusion ($\sim 2.1 \times 10^{-5}$ cm^2 s^{-1}) of O_2 in water. These transport issues restrict O_2 accessibility to the photocatalyst, limiting the overall efficiency of photocatalytic activity using conventional solid–liquid bi-phase interfaces. Additionally, such systems often suffer from poor product selectivity control, H_2O_2 decomposition, catalyst recovery difficulties, agglomeration, and limited light harvesting.

Gaseous O_2, with its higher diffusion coefficient and concentration, can replace dissolved O_2 in water to solve the problem of O_2 accessibility to the catalyst. The introduction of the new phase within the control of water state is expected to address all the discussed pending issues and significantly increase the efficiency of H_2O_2 production[16] (Table 2).

3.2.1 Photocatalytic H_2O_2 syntheses in liquid water. To solve the problem of low solubility and diffusion rate of O_2 in water, researchers have developed a variety of promising floating photocatalysts that enhance the interaction between the catalyst, O_2, and light.[77,78] For example, Lou's group designed a two-layered Janus fiber membrane (2 L-mCN/F-Naf) photocatalyst with asymmetric hydrophobicity for H_2O_2 synthesis.[21] The membrane features a highly hydrophobic polytetrafluoroethylene (PTFE) fiber bottom layer and a top layer composed of modified carbon nitride (mCN) dispersed in PTFE fibers, and treated with amphiphilic Nafion to modulate local hydrophobicity. This asymmetric structure promotes the formation of a gas–liquid–solid triple-phase interface, enabling efficient O_2 diffusion and enhancing the local concentration of reactants at the photocatalytic sites. Under visible light, the optimized membrane achieved a remarkable H_2O_2 production rate of 5.38 mmol g^{-1} h^{-1}. The design and mechanism are illustrated in Fig. 6a.

Yu's *et al.* fixed the hydrophobic TiO_2 and Bi_2O_3 on lightweight polystyrene (PS) spheres using hydrothermal and photodeposition methods.[19] By constructing an S-scheme (step-scheme) heterojunction, they achieved efficient spatial separation of photogenerated carriers, while retaining the electrons with strong reducing ability (located in the conduction band of Bi_2O_3) for the two-electron reduction of O_2 to H_2O_2, and the holes with strong oxidizing ability (located in the valence band of TiO_2) for the oxidation of organic substrates. This floating structure built a stable gas–liquid–solid three-phase interface on the solution surface, enabling the direct and rapid diffusion of gaseous O_2 to the catalyst active sites. This combination results in overcoming the bottleneck of low O_2 solubility and slow diffusion in traditional suspension systems, and improving the light utilization efficiency. The floatable S-scheme TiO_2/Bi_2O_3 photocatalyst is transparent to sunlight, achieving a significantly improved H_2O_2 yield of 1.15 mM h^{-1}, while realizing the conversion of furfuryl alcohol to furfuryl acid, as shown in Fig. 6b.

Later, the same group designed a ternary TiO_2/Pt/CoPOM floatable photocatalyst.[79] In this design, lightweight PS spheres ensured the photocatalyst floating on the liquid surface, improving light utilization and contact with the gaseous reactants. Pt and Co polyoxometalate (CoPOM) acted as a channel for electron transfer to the Pt sites through

© 2026 The Author(s). Co-published by the Institute of Process Engineering, Chinese Academy of Sciences and Royal Society of Chemistry

Open Access Article. Published on 09 April 2026. Downloaded on 4/9/2026 9:59:55 PM. This article is licensed under a Creative Commons Attribution-NonCommercial 3.0 Unported Licence.

ligand networks. This system resulted in a H_2O_2 yield of 0.93 mM h^{-1} along with a HCOOH yield of 0.46 mM h^{-1}.

Li *et al.* developed a tri-phase photocatalytic system comprising air–liquid–solid phases using polymerized carbon nitride (PCN) doped with pyrrole and cyano groups. This development boosts O_2 activation and spatially separates the HOMO and LUMO orbitals,[17] resulting in improved carrier separation efficiency and selective H_2O_2 generation. The system achieved an impressive H_2O_2 generation rate of 2063 μmol g^{-1} h^{-1} in pure water, which is about 10 times higher than that of the conventional powder photocatalyst systems.

Building on this, Kang *et al.* engineered a dual Pd/A/$BiVO_4$ photocatalyst with superhydrophobic and super-oxygenophilic properties to further enhance selectivity and suppress H_2O_2 decomposition. This tri-phase interface enabled efficient one-step two-electron O_2 reduction directly from air, significantly minimizing H_2O_2 degradation and achieving high product concentrations.[24]

3.2.2 Photocatalytic H_2O_2 synthesis in microdroplets. Microdroplet systems have recently emerged as a powerful platform for photocatalytic H_2O_2 production surpassing traditional bulk water methods. These microdroplets not only improve O_2 accessibility at the catalyst surface, but also enhance charge separation due to strong interfacial electric fields and unique solvation environments.

Zhang's group pioneered this approach by using inkjet-printed water microdroplets containing g-C_3N_4 nanosheet photocatalysts and triethanolamine as photo-generated hole scavengers.[51] The research revealed a dramatic increase in H_2O_2 generation reaching up to 20.6 mmol g^{-1} h^{-1}, which is nearly two orders of magnitude higher than conventional biphasic systems. The study also showed a volcano-type dependence on droplet size, suggesting an optimal microdroplet diameter for H_2O_2 formation. This synergistic effect, resulting from increased O_2 access, enhanced photocarrier separation, and interfacial electric fields, enabled efficient H_2O_2 production. Moreover, the team demonstrated *in situ* generation of H_2O_2 using electrospray, opening the door to portable or on-demand applications. As of now, no further studies have been reported in this area, indicating untapped potential for future experimental work.

3.2.3 Photocatalytic H_2O_2 in water vapor. To the best of our knowledge, the successful photocatalytic synthesis of H_2O_2 in water vapor environments has not yet been reported. This lack of success may be attributed to two main constraints:

(1) The thermodynamic instability of H_2O_2 in gaseous environments, which leads to spontaneous decomposition and unsustainable production (eqn (5))

$$H_2O_2 \rightarrow 2H_2O + O_2,\ \Delta G < 0 \quad (5)$$

(2) The challenge of collecting or utilizing gaseous H_2O_2 *in situ*, attributed to its high diffusivity and low concentration.

These factors, combined with the relative novelty of this approach, indicate that it remains an underexplored yet intriguing frontier in photocatalytic research.

3.3 Photocatalytic N_2 fixation

Photocatalytic N_2 fixation involves converting atmospheric N_2 into plant-available ammonia (NH_3), nitrate, or urea, contributing to renewable nitrogen energy production. By harnessing sunlight, this process demonstrates high efficiency and sustainability, which can enhance crop growth and reduce reliance on chemical fertilizers. However, conventional solid–liquid bi-phase photocatalytic systems, where the photocatalyst surface is fully immersed in water, face two significant challenges:

(1) The poor solubility and slow diffusion rate of N_2 severely restrict its N_2 availability at the catalyst surface.

(2) The two-electron HER reactions compete for photogenerated electrons, which undermines the multi-electron transfer required for effective N_2 fixation.

To overcome these challenges, recent studies have been focusing on engineering gas–liquid–solid interfaces. In this section, we discuss the positive results in photocatalytic N_2 fixation under three different water states.

3.3.1 Photocatalytic N_2 fixation in liquid water. Enhancing N_2 fixation efficiency in liquid water can be achieved by designing floatable platforms or modifying the wettability of photocatalysts, ensuring direct exposure to a N_2 atmosphere while remaining in contact with water.

For example, to address the low solubility of N_2 in water and the liquid-phase diffusion coefficient, Li *et al.* designed a floating photocatalyst (Bi/CC) by loading metallic bismuth (Bi) onto carbon cloth. During the synthesis, polyvinylpyrrolidone (PVP) was implemented as a surfactant and structure-directing agent, performing several functions, which regulated Bi crystallinity and morphology. At an optimal amount of 1.0 g, it forms regular hollow spheres with high crystallinity, the highest specific surface area, and the strongest N_2 adsorption capacity. The wettability of the carbon cloth substrate is intrinsically determined by its hydrophilic or hydrophobic nature, enabling the construction of a stable gas–liquid–solid triphase interface for direct N_2 supply to catalytic sites when using hydrophilic carbon cloth. While placing the photocatalyst directly in an N_2 atmosphere, the carbon cloth substrate enhances photothermal heating, promoting N_2 activation at the interface, and yielding an impressive rate of 2.85 mmol L^{-1} h^{-1} g^{-1} for NH_3, which is four times higher than what is achievable in a conventional biphasic system.[80] The comparison of the results from diphase and triphase systems is presented in Fig. 7a.

Liu's team developed a hydrophilic–hydrophobic structure by depositing hydrophilic $Bi_4O_5Br_2$ onto a hydrophobic ZIF-8 surface. This tri-phase interface, ensured by the wettability contrast, promoted a rapid N_2 supply and effective capture of photogenerated electrons, resulting in 327 μmol L^{-1} h^{-1} g^{-1}

© 2026 The Author(s). Co-published by the Institute of Process Engineering, Chinese Academy of Sciences and Royal Society of Chemistry

Open Access Article. Published on 09 April 2026. Downloaded on 4/9/2026 9:59:55 PM.
This article is licensed under a Creative Commons Attribution-NonCommercial 3.0 Unported Licence.

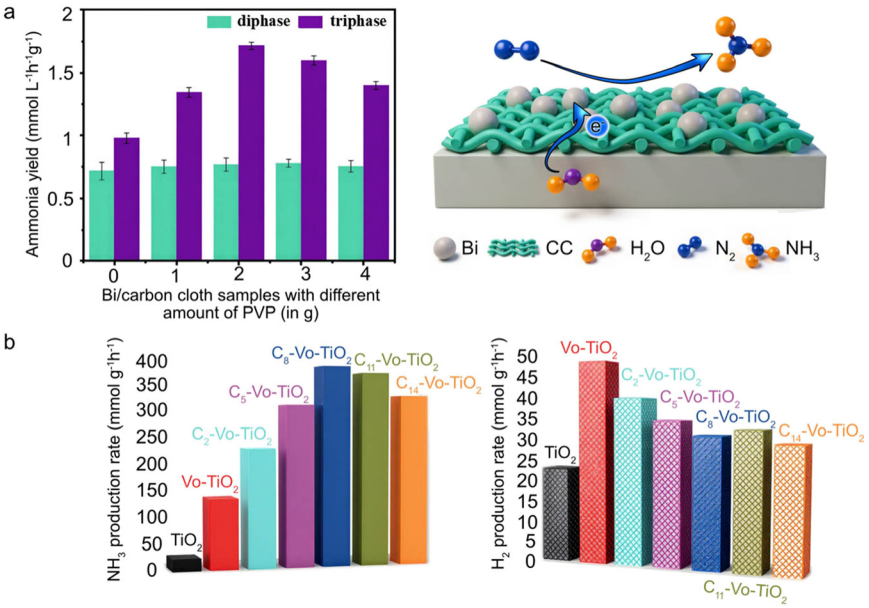

Fig. 7 Demonstrations of photocatalytic N_2 fixation in liquid water. (a) Comparison of ammonia yields from bi/carbon cloth using diphase and triphase systems, along with a schematic illustration of the photocatalytic N_2 reduction reaction at a gas–liquid–solid interface. Reprinted with permission from ref. 80. Copyright 2022, Royal Society of Chemistry; (b) NH_3 and H_2 production rates achieved using alkyl-acid-modified TiO_2 photocatalysts, highlighting the influence of carbon chain length on selectivity and activity. Reprinted with permission from ref. 23. Copyright 2023, Tsinghua University Press.

of NH_3, which is 3.6 times greater than that of $Bi_4O_5Br_2$ alone.[81]

In a separate study, Guan *et al.* modified the surface of defective TiO_2 by using alkyl acids with different carbon chain lengths. This optimization enhanced the catalyst's wettability and established a gas–liquid–solid tri-phase interface increasing N_2 adsorption at oxygen-vacancy sites while suppressing the HER. The NH_3 production rate for *n*-octanoic acid-deficient TiO_2 reached 392 μmol g^{-1} h^{-1}.[23] The influence of wettability adjustment on the production yields and selectivity is summarized in Fig. 7b.

3.3.2 Photocatalytic N_2 fixation in microdroplets. In theory, microdroplet reactors suspend ultrafine water droplets in a N_2 atmosphere, creating highly curved gas–liquid interfaces that concentrate N_2 around catalyst particles and generate interfacial electric fields that enhance charge separation. Although there have been no direct demonstrations of N_2 fixation in microdroplets, recent research indicates significant potential in this approach.

For example, Zare's group used an ultrasonic spray to produce microdroplets of water mixed with N_2 and CO_2 over a solid-phase graphite carrier network loaded with $CuBi_2O_4$ for urea synthesis. They achieved 2.8 ± 0.3 μM concentration detected by real-time mass spectrometry.[54] In this system, the microdroplets act as both a transport medium for gaseous reactants and as proton/electron donors for urea synthesis. By replacing $CuBi_2O_4$ with an N_2-selective photocatalyst under illumination, it is possible to reach similar or even enhanced N_2 fixation efficiency. Moreover, we hypothesize that N_2 fixation could also be realized by using a similar system to the one developed by Zhang *et al.* for microdroplet-coupled photocatalytic H_2O_2 synthesis or CO_2RR.[51]

3.3.3 Photocatalytic N_2 fixation in water vapor. Operating in a water vapor environment eliminates solvent flooding, allowing direct contact between the catalyst, gaseous N_2, and water vapor. This configuration not only inhibits the HER, but also solves the issue of insufficient N_2 supply. In addition, the photothermal and hydrovoltaic effects at the solid–gas interface further drive charge separation.

Following this development, Meng's group constructed a tri-phase interfacial system for photocatalytic NH_3 production by immobilizing TiO_2 on hydrophilic carbon paper, and exposing it to N_2.[82] This system achieved an NH_3 production rate of 360.37 μmol g^{-1} h^{-1}, which is 21 times higher than the yield from a conventional bi-phase interfacial system. During outdoor sunlight tests, the system produced NH_3 at a rate of 73.65 μmol g^{-1} h^{-1} demonstrating the potential for large-scale photocatalytic N_2 fixation. Using a related strategy, Lu's group coupled metal-phthalocyanine-derived porous organic frameworks (POFs) with a novel gas-dominated interface.[83] This system overturns the traditional "gas in solvent" three-phase reaction mode and creates a "solvent in gas" system, with the reaction gas (such as N_2) as the dominant environment. Specifically: the photocatalyst is directly placed in the flowing nitrogen gas, while the proton source (such as water/methanol) is ultrasonically atomized and uniformly suspended in the gas atmosphere in the form of micro-nano droplets. This design brings two core advantages. On the one hand, enhanced mass transfer: the diffusion coefficient of nitrogen gas in the gas phase is nearly three orders of magnitude higher than in the liquid phase,

© 2026 The Author(s). Co-published by the Institute of Process Engineering, Chinese Academy of Sciences and Royal Society of Chemistry

Open Access Article. Published on 09 April 2026. Downloaded on 4/9/2026 9:59:55 PM.
This article is licensed under a Creative Commons Attribution-NonCommercial 3.0 Unported Licence.

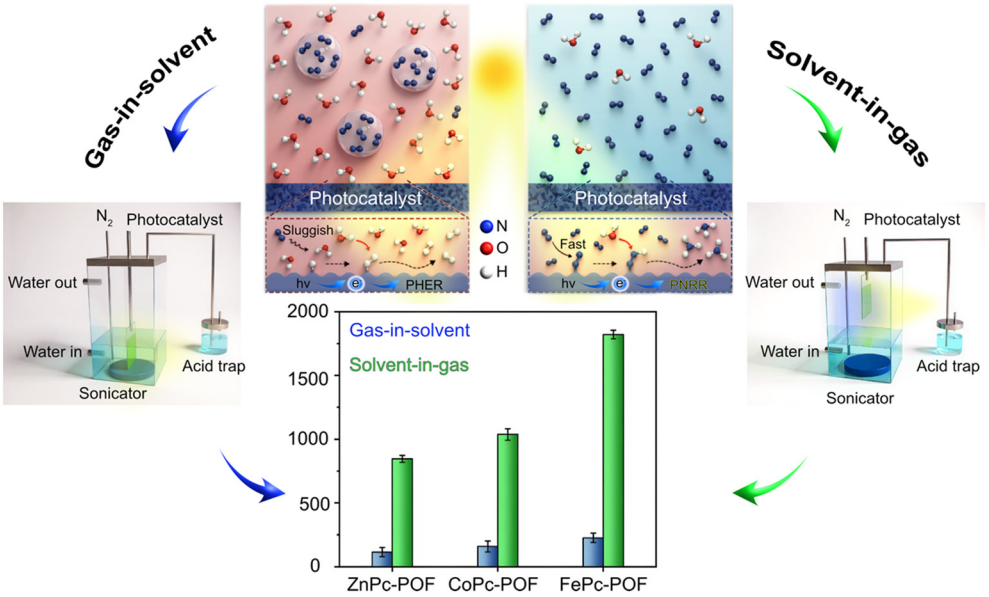

Fig. 8 Schematic illustration of experimental setups and reaction mechanisms using conventional gas-in-solid and advanced solid-to-gas systems, indicating the significant increase in photocatalytic NH_3 synthesis. Reprinted with permission from ref. 83. Copyright 2023, Wiley-VCH GmbH.

enabling the porous framework to efficiently adsorb and enrich high-concentration N_2 molecules; on the other hand, inhibition of side reactions: the contact between the catalyst surface and the bulk solvent is significantly limited, effectively suppressing the competitive hydrogen evolution reaction caused by excess water. This strategy increases the ammonia production rate of photocatalysis to over 1820.7 μmol g^{-1} h^{-1}, which is more than eight times higher than the traditional system, and the apparent quantum efficiency at 400 nm is 0.5%. These impressive results are shown in Fig. 8.

3.4 Summary

As systematically demonstrated in section 3, phase-interface engineering through the control of water's physical state is a practically-oriented strategy to overcome the mass-transport, selectivity, and charge-dynamics challenges of conventional photocatalysis. Through rational interface design and optimized material combinations, researchers have achieved significant breakthroughs in three critical application areas.

In CO_2RR, tri-phase interfaces in aqueous systems dramatically boost CO_2 availability at active sites while simultaneously suppressing the HER and steering selectivity toward valuable products. Microdroplet reactors offer dual advantages: (1) local CO_2 enrichment and (2) intense interfacial electric fields that promote charge separation. Remarkably, gas–solid interfaces under humid conditions enable ultra-selective synthesis of target chemicals with ultra-high selectivity, demonstrating the transformative potential of phase engineering.

In H_2O_2 synthesis, phase-engineered systems, including floating photocatalysts, microdroplets, or vapor interfaces raise local O_2 concentration, which inhibits H_2O_2 decomposition. These advantages improve selectivity, increase yields, suppress the HER, and optimize charge-carrier dynamics, moving photocatalytic H_2O_2 synthesis closer to large-scale practical applications.

For N_2 fixation, floating and wettability-tuned catalysts in liquid water create tri-phase interfaces that facilitate direct delivery of N_2 from the gas phase, while suppressing the HER. Vapor-phase interfaces further leverage photothermal and hydrovoltaic effects to dramatically improve charge separation efficiency. While microdroplet-mediated N_2 fixation remains unexplored, its inherent ability to concentrate gaseous reactants and amplify interfacial fields presents an exciting research frontier. Notably, the photocatalytic synthesis of higher-value nitrogen compounds (urea, nitrates) through phase interface regulation remains completely unreported – a promising area for future research aimed at advancing photocatalytic N_2 fixation.

Across all these reactions, phase-interface modulation consistently improves photocatalytic performance by (1) ensuring effective gas-phase supply of CO_2, O_2, or N_2; (2) suppressing the HER; (3) regulating product selectivity; and (4) enhancing photogenerated charge separation and utilization.

4 Characterization methods for probing mechanisms at phase interfaces

Understanding the reasons behind the enhanced photocatalytic performance at water-state-modulated phase

© 2026 The Author(s). Co-published by the Institute of Process Engineering, Chinese Academy of Sciences and Royal Society of Chemistry

Open Access Article. Published on 09 April 2026. Downloaded on 4/9/2026 9:59:55 PM. This article is licensed under a Creative Commons Attribution-NonCommercial 3.0 Unported Licence.

interfaces requires moving beyond conventional solid–liquid catalyst characterization. The unique interfacial environment conditions, including intense spontaneous electric fields in microdroplets, localized reactant enrichment at triphase boundaries, and synergistic photothermal/hydrovoltaic effects at gas–solid interfaces, demand the choice of adequate characterization techniques. This section provides a systematic overview of the experimental and theoretical methods that have proven to be the most powerful for resolving structure–activity relationships and dynamic mechanisms at these advanced interfaces, providing a toolbox for future research in this field.[46–48]

4.1 Probing interfacial structure and microenvironment

First of all, it is important to reveal the morphology and physicochemical properties of the interfaces. Scanning electron microscopy (SEM) and transmission electron microscopy (TEM) remain the standards for visualizing the microstructure, including the morphology of floatable PS-sphere-supported composites and the distribution of active sites.[15,19] X-ray photoelectron spectroscopy (XPS) complements morphological analysis by resolving the oxidation states and chemical bonding environments of surface species. Contact angle measurements, in turn, quantitatively define the wettability of catalyst surfaces, directly correlating hydrophobicity/hydrophilicity with the ability to form stable gas–liquid–solid triphase interfaces, as demonstrated in studies on alkyl-acid-modified TiO_2 (ref. 23) and Janus fiber membranes.[21]

Brunauer–Emmett–Teller (BET) surface area analysis evaluates the porosity of scaffold materials (*e.g.*, carbon cloth, porous frameworks), which governs gaseous reactant adsorption and diffusion in vapor-phase or "solvent-in-gas" (SIG) systems.[83] For microdroplet systems specifically, dynamic light scattering (DLS) is a commonly used tool to determine the droplet size distribution, which is a key parameter influencing interfacial curvature and field strength.[52,55]

4.2 Elucidating charge carrier dynamics

Prior to the investigation of the charge behavior, it is critical to understand whether an interfacial electric field exists and to quantify its magnitude, since such fields are the primary drivers of enhanced separation in microdroplet systems. This could be evaluated by Vibrational Stark effect spectroscopy, particularly using surface-enhanced Raman scattering (SERS) with molecular probes (*e.g.*, 4-nitrobenzenethiol or SCN^-). This is a powerful tool to directly measure and map the immense electric field ($\sim 10^8$–10^9 V m^{-1}) at the air–water interface of microdroplets.[30]

Steady-state and time-resolved photoluminescence (PL) spectroscopy are great methods to reveal the efficiency of electron–hole pair separation and their recombination lifetimes. Significant PL quenching and prolonged lifetimes often indicate effective charge separation facilitated by interfacial fields or heterojunctions, as could be seen in S-scheme TiO_2/Bi_2O_3 systems.[19] Transient photocurrent response and electrochemical impedance spectroscopy (EIS) performed on electrode-immobilized catalysts provide insights into charge transfer resistance and conductivity at the phase interface.[65,79]

For processes occurring on the ultrafast timescale, femtosecond transient absorption (fs-TA) spectroscopy is indispensable. By tracking the ultrafast kinetics of photogenerated charge carriers on picosecond to nanosecond timescales, fs-TA promotes the understanding of the initial separation events driven by interfacial electric fields in microdroplet systems.[19,61]

4.3 Monitoring reaction dynamics and intermediates

Identifying the molecular intermediates that are formed and transformed at the phase interface under operating conditions is essential for establishing the mechanisms. *In situ* Fourier-transform infrared (FTIR) or diffuse reflectance infrared Fourier-transform spectroscopy (DRIFTS) both allow real-time observation of adsorbed reactants and key reaction intermediates (*e.g.*, *COOH for CO_2 reduction, *N_2H for N_2 fixation) on the catalyst surface.[19,83] Isotope tracer experiments (*e.g.*, using $^{13}CO_2$ or $^{15}N_2$) coupled with mass spectrometry (MS) or nuclear magnetic resonance (NMR) are definitive methods to confirm the origin of products, ruling out carbon or nitrogen sources from contaminants, as rigorously applied in studies on CO_2 reduction and N_2 fixation.[52,83]

Experimental observations are most powerfully interpreted when supported by theoretical modeling. Thus, density functional theory (DFT) calculations simulate adsorption energies, reaction pathways, and activation barriers at model interfaces. DFT is essential for verifying the role of interfacial fields in lowering energy barriers and predicting catalyst design principles.[19,51,71]

4.4 Quantifying macroscopic system effects

The unique energy conversion pathways in water-state-driven systems (particularly photothermal heating and hydrovoltaic potential generation) require dedicated macroscopic characterization tools. Infrared thermal imaging, in this regard, provides spatially resolved temperature maps of catalyst surfaces under illumination, directly quantifying the photothermal contribution in systems such as Bi/carbon cloth and enabling its correlation with catalytic activity.[80] Open-circuit voltage and short-circuit current measurements, in turn, directly quantify the electrical output from hydrovoltaic or evaporation-induced potential generation, as exemplified in PAA/CoO-NC and related systems.[64,65]

Reliable quantification of catalytic output requires the appropriate analysis for each target product. Gas chromatography (GC), high-performance liquid

© 2026 The Author(s). Co-published by the Institute of Process Engineering, Chinese Academy of Sciences and Royal Society of Chemistry

Open Access Article. Published on 09 April 2026. Downloaded on 4/9/2026 9:59:55 PM.
This article is licensed under a Creative Commons Attribution-NonCommercial 3.0 Unported Licence.

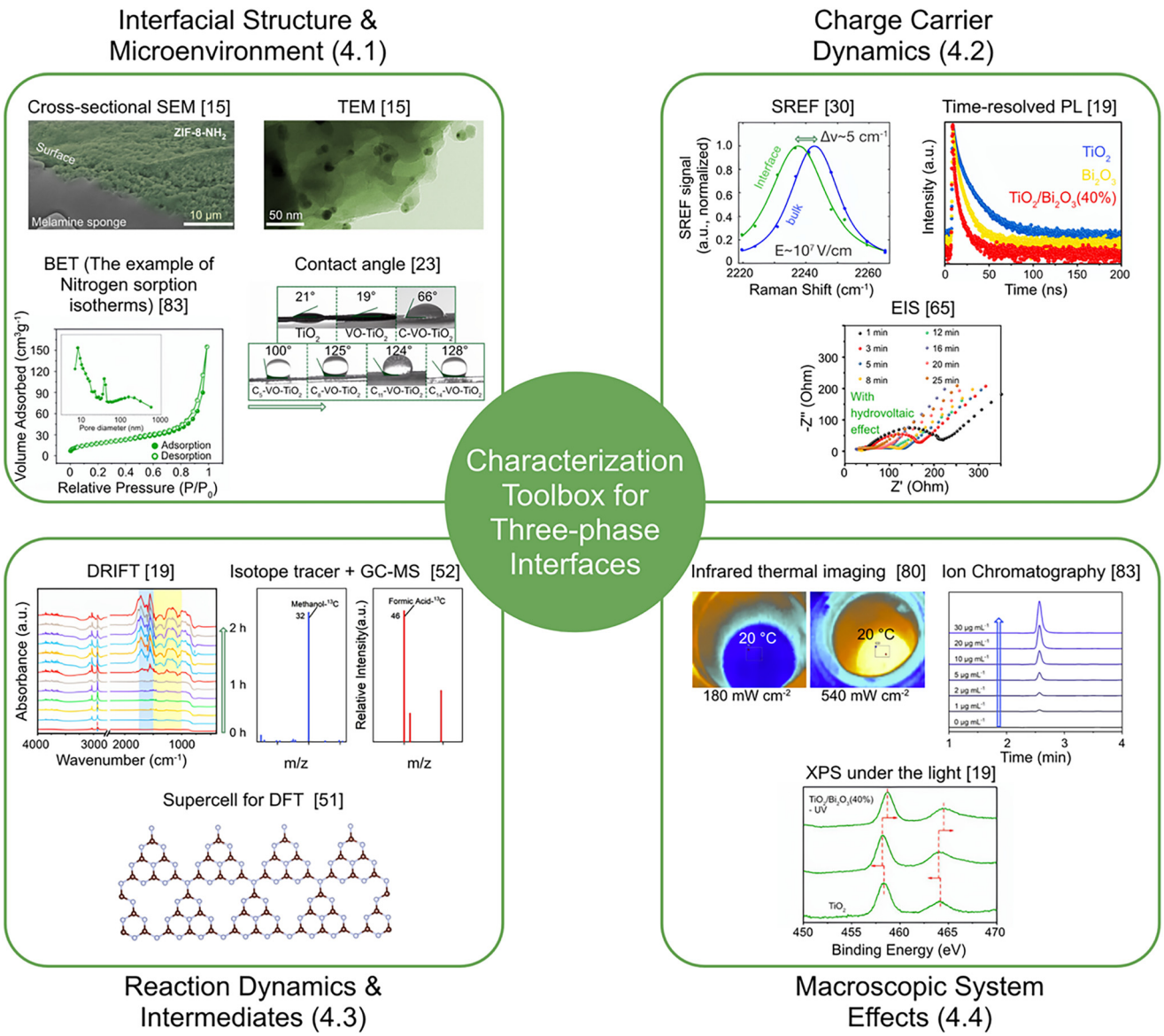

Fig. 9 Multi-modal characterization framework for probing mechanisms at water-state-modulated phase interfaces, summarizing the methods introduced in subsections. Reprinted with permission from ref. 15. Copyright 2025, Springer Nature; reprinted with permission from ref. 19. Copyright 2022, Wiley-VCH GmbH; reprinted with permission from ref. 23. Copyright 2023, Tsinghua University Press; reprinted with permission from ref. 30. Copyright 2020, American Chemical Society; reprinted with permission from ref. 51. Copyright 2023, The Royal Society of Chemistry; reprinted with permission from ref. 52. Copyright 2023, Wiley-VCH GmbH; reprinted with permission from ref. 65. Copyright 2023, Springer Nature; reprinted with permission from ref. 80. Copyright 2022, The Royal Society of Chemistry; reprinted with permission from ref. 83. Copyright 2023, Wiley-VCH GmbH.

chromatography (HPLC), and ion chromatography (IC) represent the standard techniques for quantifying gaseous and liquid products (*e.g.*, CO, CH_4, H_2O_2, NH_4^+).[51,83] Long-term cyclic tests coupled with post-reaction characterizations (XRD, XPS) assess the stability and extended cycling tests of the interfacial systems.[19,51]

Together, this integrated multi-modal characterization framework provides the analytical foundation to bridge the gap between macroscopic performance metrics and microscopic interfacial mechanisms, guiding the rational design of next-generation phase-engineered photocatalytic systems in Fig. 9.

5 Summary and outlook

5.1 Summary

In this review article, we demonstrate that controlling water states to modulate phase interfaces is an effective strategy for enhancing the efficiency of photocatalytic reactions involving Earth's abundant small gaseous molecules.

In liquid water, designing floating photocatalysts and adjusting their hydrophobicity creates gas–liquid–solid tri-phase interfaces. This approach addresses challenges such as light shielding, scattering, and the low solubility and slow

Open Access Article. Published on 09 April 2026. Downloaded on 4/9/2026 9:59:55 PM. This article is licensed under a Creative Commons Attribution-NonCommercial 3.0 Unported Licence.

diffusion rates of gaseous molecules in conventional biphasic systems.

For microdroplets, dispersing photocatalysts within droplets or spraying them onto carriers leverages the intense electric field at the droplet surface. This approach drives photogenerated charge separation overcoming the limitations of conventional interfaces.

In water vapor, photocatalysts are often combined with photothermal materials that float on the water surface to generate vapor through the photothermal effect. The can also be suspended in a vapor atmosphere with reactive small molecules.

These innovative solutions provide a robust platform for optimizing photocatalytic reaction kinetics, opening new opportunities for industrial applications in the environmental and energy sectors.

5.2 Future outlook

Despite significant progress, the implementation of novel interfaces for photocatalytic applications remains challenging. Below are key issues and future perspectives:

(1) Reactor design for real-world applications. The productivity of photocatalysis is directly proportional to the illuminated area. Currently, both traditional biphasic systems and emerging phase interfaces are limited to small-scale reactors, which do not meet real real-world needs. Developing large-scale reactors tailored for different phase interfaces is essential to fulfill practical demands.

(2) Developing multifunctional photocatalysts suitable for emerging phase interfaces. Multifunctional materials have significant potential. For instance, photothermal materials can absorb infrared light under solar illumination and convert it into thermal energy to boost charge separation, which is not accessible to traditional photocatalysts. Similarly, photocatalysts with piezoelectric properties can enhance charge separation when exposed to ultrasound. By integrating photocatalysis with piezoelectric and photothermal effects, we can improve light absorption, charge separation, transfer, and mass transfer, ultimately boosting reaction kinetics and overall photocatalytic performance.

(3) Expanding to unexplored photocatalytic reactions at emerging phase interfaces. Currently, only a few photocatalytic reactions have been systematically studied in these emerging interface systems, leaving the potential to implement more in the upcoming studies. Future concepts should focus on expanding the application scope of interface engineering and exploring its potential in more reaction systems. For example, in the case of droplets, there are no systematic studies on photocatalytic N_2 fixation, overall water splitting, organic synthesis, and pollutant degradation; while for the water vapor system, the synthesis of H_2O_2 is still missing. Systematic investigation of these reactions, combined with *in situ* characterization to elucidate charge transfer mechanisms, optimized microreactor designs, and surface engineering of catalytic materials, could lead to significant efficiency breakthroughs and support industrial-scale applications of new reactions.

(4) Direct *in situ* utilization of products in agriculture. The *in situ* use of photogenerated products in agriculture presents substantial advantages, simplifying extraction and purification processes while boosting food production. Unlike electrocatalysis, which requires electrolytes, photocatalytic reactions in aqueous media can directly produce valuable outputs. For instance, nitrogenous products from N_2 fixation (such as NH_4^+, NO_3^-, and urea) can serve as fertilizers, applied through drip-irrigation into the soil to promote plant photosynthesis. Additionally, H_2O_2 photocatalytic synthesis can be used *in situ* for seed germination, soil sterilization, plant growth and alleviation of non-biological stress. Liquid products resulting from CO_2RR, such as formic acid and ethanol, can also serve as growth regulators to promote plant development. To achieve direct *in situ* utilization of photocatalytic products in agriculture, the issues of separation and toxicity must be addressed through both materials and system design. First, developing highly efficient catalysts composed entirely of non-toxic elements is essential for safe three-phase interface operation. Second, it is of high importance to construct a new type of reactor that enables effective physical separation of the catalyst from the target product. Although both of these points represent significant challenges, addressing catalyst safety and separation cannot be ignored if photocatalytic systems are to find practical application in agricultural production.

(5) Addressing specific challenges of each interface type to improve scalability for practical applications. A fundamental challenge common to all gas–liquid–solid triphase systems is maintaining stable interfaces during extended operation. For example, floating catalysts can aggregate or sink over time due to changes in surface wettability caused by fouling, while hydrophobic coatings may degrade under prolonged UV irradiation or oxidative conditions. Scaling up requires engineering solutions for catalyst immobilization, continuous product removal, and bio-fouling prevention. Microdroplet photocatalysis currently relies on aerosol generators or spray nozzles, which produce relatively low throughput, making continuous industrial-scale operation time-consuming and economically challenging. Additionally, individual microdroplets have short lifetimes (milliseconds to seconds) before coalescence or evaporation occurs. Thus, more advanced systems for droplet generation and stabilization need to be developed. Water vapor systems require precise humidity control and face thermal management challenges. The need for continuous vapor generation (either through photothermal heating or external humidification) adds complexity and energy costs. Furthermore, catalyst stability under oscillating humidity conditions has not been thoroughly evaluated over the extended operation periods (months to years) required for practical deployment. Overall, most practical challenges stem from uncertainties in long-

© 2026 The Author(s). Co-published by the Institute of Process Engineering, Chinese Academy of Sciences and Royal Society of Chemistry

Open Access Article. Published on 09 April 2026. Downloaded on 4/9/2026 9:59:55 PM. This article is licensed under a Creative Commons Attribution-NonCommercial 3.0 Unported Licence.

term stability and the need to engineer robust equipment suitable for both laboratory research and industrial implementation. Nevertheless, the performance potential demonstrated by these emerging interfaces justifies continued efforts to develop novel solutions in this area.

Conflicts of interest

The authors declare no conflict of interest.

Data availability

No primary research results, software or code have been included and no new data were generated or analysed as part of this review.

Acknowledgements

This study was mainly supported by the National Natural Science Foundation of China (Grant No. 22308223), the High-level Talents launching Project (RCZK202328), and Xinjiang Uygur Autonomous Region Tianchi Talent Introduction Program (Young Doctor) for Bin Yang.

References

1 D. Cheng, Solar and wind, *Nat. Clim. Change*, 2023, **13**, 1020–1020.
2 R. Li, Photocatalytic nitrogen fixation: An attractive approach for artificial photocatalysis, *Chin. J. Catal.*, 2018, **39**, 1180–1188.
3 H. Jiao, C. Wang, L. Xiong and J. Tang, Insights on carbon neutrality by photocatalytic conversion of small molecules into value-added chemicals or fuels, *Acc. Mater. Res.*, 2022, **3**, 1206–1219.
4 A. Fujishima and K. Honda, Electrochemical photolysis of water at a semiconductor electrode, *Nature*, 1972, **238**, 37–38.
5 H. Nishiyama, T. Yamada, M. Nakabayashi, Y. Maehara, M. Yamaguchi, Y. Kuromiya, Y. Nagatsuma, H. Tokudome, S. Akiyama, T. Watanabe, R. Narushima, S. Okunaka, N. Shibata, T. Takata, T. Hisatomi and K. Domen, Photocatalytic solar hydrogen production from water on a 100-m^2 scale, *Nature*, 2021, **598**, 304–307.
6 Y. Zhao, C. Ding, J. Zhu, W. Qin, X. Tao, F. Fan, R. Li and C. Li, A hydrogen farm strategy for scalable solar hydrogen production with particulate photocatalysts, *Angew. Chem., Int. Ed.*, 2020, **59**, 9653–9658.
7 L. Liu, J. Hu, Z. Ma, Z. Zhu, B. He, F. Chen, Y. Lu, R. Xu, Y. Zhang, T. Ma, M. Sui and H. Huang, One-dimensional single atom arrays on ferroelectric nanosheets for enhanced CO_2 photoreduction, *Nat. Commun.*, 2024, **15**, 305.
8 H. Li, Y. Zhang, J. Li, Q. Liu, X. Zhang, Y. Zhang and H. Huang, Boosting H_2O_2 evolution of CdS via constructing a ternary photocatalyst with earth-abundant halloysite nanotubes and NiS co-catalyst, *Chin. J. Catal.*, 2025, **69**, 111–122.
9 Z. Zhu, J. Hu, C. Hu, Y. Lu, S. Chu, F. Chen, Y. Zhang and H. Huang, Oriented crystal polarization tuning bulk charge and single-site chemical state for exceptional hydrogen photoproduction, *Adv. Mater.*, 2024, **36**, 2411339.
10 Q.-S. Huang, C. Chu, Q. Li, Q. Liu, X. Liu, J. Sun, B.-J. Ni and S. Mao, Three-phase interface construction on hydrophobic carbonaceous catalysts for highly active and selective photocatalytic CO_2 conversion, *ACS Catal.*, 2023, **13**, 11232–11243.
11 H. Zhou, X. Sheng, Z. Ding, X. Chen, X. Zhang, X. Feng and L. Jiang, Liquid–liquid–solid triphase interface microenvironment mediates efficient photocatalysis, *ACS Catal.*, 2022, **12**, 13690–13696.
12 C. He, L. Shang, H. Zhu, L. Yu, L. Wang and J. Zhang, Photocatalytic conversion of methane to ethanol at a three-phase interface with concentration-matched hydroxyl and methyl radicals, *J. Am. Chem. Soc.*, 2024, **146**, 11968–11977.
13 Y. Guo, Y. Dong, B. Liu, B. Ni, C. Pan, J. Zhang, H. Zhao, G. Wang and Y. Zhu, Effective H_2O_2 photosynthesis in gas–liquid–solid triphase system with self-floating conjugated organic polymers, *Adv. Funct. Mater.*, 2024, **34**, 2402920.
14 Y. Xie, M. Wang, Q. Huang, Q. Huang, B. Sheng, W. Song, H. Sheng and J. Zhao, A floatable photocatalyst to synergistically promote CO_2 reduction and water oxidation by creating oriented charge separation across a tri-phase interface, *Energy Environ. Sci.*, 2024, **17**, 4725–4734.
15 J. Wang, J. Zhang, Y. Li, X. Xia, H. Yang, J.-H. Kim and W. Zhang, Silver single atoms and nanoparticles on floatable monolithic photocatalysts for synergistic solar water disinfection, *Nat. Commun.*, 2025, **16**, 981.
16 L. Li, L. Xu, Z. Hu and J. C. Yu, Enhanced mass transfer of oxygen through a gas–liquid–solid interface for photocatalytic hydrogen peroxide production, *Adv. Funct. Mater.*, 2021, **31**, 2106120.
17 S. Yan, Y. Li, X. Yang, X. Jia, J. Xu and H. Song, Photocatalytic H_2O_2 generation reaction with a Benchmark Rate at air-liquid-solid joint interfaces, *Adv. Mater.*, 2024, **36**, 2307967.
18 W. H. Lee, C. W. Lee, G. D. Cha, B.-H. Lee, J. H. Jeong, H. Park, J. Heo, M. S. Bootharaju, S.-H. Sunwoo, J. H. Kim, K. H. Ahn, D.-H. Kim and T. Hyeon, Floatable photocatalytic hydrogel nanocomposites for large-scale solar hydrogen production, *Nat. Nanotechnol.*, 2023, **18**, 754–762.
19 B. He, Z. Wang, P. Xiao, T. Chen, J. Yu and L. Zhang, Cooperative coupling of H_2O_2 production and organic synthesis over a floatable polystyrene-sphere-supported TiO_2/Bi_2O_3 S-scheme photocatalyst, *Adv. Mater.*, 2022, **34**, 2203225.
20 Z. Zhang, Y. Wang, Y. Xie, T. Tsukamoto, Q. Zhao, Q. Huang, X. Huang, B. Zhang, W. Song, C. Chen, H. Sheng and J. Zhao, Floatable artificial leaf to couple oxygen-tolerant CO_2 conversion with water purification, *Nat. Commun.*, 2025, **16**, 274.
21 Y. Li, Z. Pei, D. Luan and X. W. D. Lou, Triple-phase photocatalytic H_2O_2 production on a Janus fiber membrane

© 2026 The Author(s). Co-published by the Institute of Process Engineering, Chinese Academy of Sciences and Royal Society of Chemistry

Open Access Article. Published on 09 April 2026. Downloaded on 4/9/2026 9:59:55 PM.
This article is licensed under a Creative Commons Attribution-NonCommercial 3.0 Unported Licence.

with asymmetric hydrophobicity, *J. Am. Chem. Soc.*, 2024, **146**, 3343–3351.

22 X. Sheng, Z. Liu, R. Zeng, L. Chen, X. Feng and L. Jiang, Enhanced photocatalytic reaction at air–liquid–solid joint interfaces, *J. Am. Chem. Soc.*, 2017, **139**, 12402–12405.

23 R. Guan, X. Cheng, Y. Chen, Z. Wu, Z. Zhao, Q. Shang, Y. Sun and Z. Sun, Wettability control of defective TiO_2 with alkyl acid for highly efficient photocatalytic ammonia synthesis, *Nano Res.*, 2023, **16**, 10770–10778.

24 M. Sun, X. Wang, Y. Li, H. Pan, M. Murugananthan, Y. Han, J. Wu, M. Zhang, Y. Zhang and Z. Kang, Bifunctional Pd-Ox center at the liquid–solid–gas triphase interface for H_2O_2 photosynthesis, *ACS Catal.*, 2022, **12**, 2138–2149.

25 Y. Zhang, H. Zhang, F. Chang, P. Xie, Q. Liu, L. Duan, H. Wu, X. Zhang, W. Peng, F. Liu and L. Xu, In-situ responses of phytoplankton to graphene photocatalysis in the eutrophic lake Xingyun, southwestern China, *Chemosphere*, 2021, **278**, 130489.

26 Z. Chen, H. Weng, C. Chu, D. Yao, Q. Li, C. Zhang and S. Mao, Nitrogen heterocyclic covalent organic frameworks for efficient H_2O_2 photosynthesis and in situ water treatment, *Nat. Commun.*, 2025, **16**, 6943.

27 M. Li, C. Boothby, R. E. Continetti and V. H. Grassian, Size-dependent sigmoidal reaction kinetics for pyruvic acid condensation at the air–water interface in aqueous microdroplets, *J. Am. Chem. Soc.*, 2023, **145**, 22317–22321.

28 K. Gong, J. Ao, K. Li, L. Liu, Y. Liu, G. Xu, T. Wang, H. Cheng, Z. Wang, X. Zhang, H. Wei, C. George, A. Mellouki, H. Herrmann, L. Wang, J. Chen, M. Ji, L. Zhang and J. S. Francisco, Imaging of pH distribution inside individual microdroplet by stimulated Raman microscopy, *Proc. Natl. Acad. Sci. U. S. A.*, 2023, **120**, e2219588120.

29 H. Hao, I. Leven and T. Head-Gordon, Can electric fields drive chemistry for an aqueous microdroplet?, *Nat. Commun.*, 2022, **13**, 280.

30 H. Xiong, J. K. Lee, R. N. Zare and W. Min, Strong electric field observed at the interface of aqueous microdroplets, *J. Phys. Chem. Lett.*, 2020, **11**, 7423–7428.

31 Q. Liang, C. Zhu and J. Yang, Water charge transfer accelerates criegee intermediate reaction with H_2O – radical anion at the aqueous interface, *J. Am. Chem. Soc.*, 2023, **145**, 10159–10166.

32 Y. Liu, Q. Ge, T. Wang, R. Zhang, K. Li, K. Gong, L. Xie, W. Wang, L. Wang, W. You, X. Ruan, Z. Shi, J. Han, R. Wang, H. Fu, J. Chen, C. K. Chan and L. Zhang, Strong electric field force at the air/water interface drives fast sulfate production in the atmosphere, *Chem*, 2024, **10**, 330–351.

33 S. Shaik, R. Ramanan, D. Danovich and D. Mandal, Structure and reactivity/selectivity control by oriented-external electric fields, *Chem. Soc. Rev.*, 2018, **47**, 5125–5145.

34 V. V. Welborn, L. R. Pestana and T. Head-Gordon, Computational optimization of electric fields for better catalysis design, *Nat. Catal.*, 2018, **1**, 649–655.

35 L. Xu, E. I. Izgorodina and M. L. Coote, Ordered solvents and ionic liquids can be harnessed for electrostatic catalysis, *J. Am. Chem. Soc.*, 2020, **142**, 12826–12833.

36 K. Gong, Y. Meng, R. N. Zare and J. Xie, Molecular mechanism for converting carbon dioxide surrounding water microdroplets containing 1,2,3-triazole to formic acid, *J. Am. Chem. Soc.*, 2024, **146**, 8576–8584.

37 J. Zhou, Q. Wang, G. Cheng, W. Shen, R. N. Zare and X. Sun, Charged water microdroplets enable dissociation of surrounding dioxygen, *J. Am. Chem. Soc.*, 2025, **147**, 10916–10924.

38 K. Li, B. Zhang, D. Xia, Z. Ye, Y. Pan, J. S. Francisco and Z. Mi, Room-temperature catalyst-free ammonia decomposition for hydrogen production on water microdroplets, *J. Am. Chem. Soc.*, 2025, **147**, 20417–20425.

39 J. K. Lee, K. L. Walker, H. S. Han, J. Kang, F. B. Prinz, R. M. Waymouth, H. G. Nam and R. N. Zare, Spontaneous generation of hydrogen peroxide from aqueous microdroplets, *Proc. Natl. Acad. Sci. U. S. A.*, 2019, **116**, 19294–19298.

40 Z. Song, C. Liang, K. Gong, S. Zhao, X. Yuan, X. Zhang and J. Xie, Harnessing the high interfacial electric fields on water microdroplets to accelerate Menshutkin reactions, *J. Am. Chem. Soc.*, 2023, **145**, 26003–26008.

41 J. Wang, D. Huang, F. Chen, J. Chen, H. Jiang, Y. Zhu, C. Chen and J. Zhao, Rapid redox cycling of Fe(II)/Fe(III) in microdroplets during iron–citric acid photochemistry, *Environ. Sci. Technol.*, 2023, **57**, 4434–4442.

42 C. Gong, D. Li, X. Li, D. Zhang, D. Xing, L. Zhao, X. Yuan and X. Zhang, Spontaneous reduction-induced degradation of viologen compounds in water microdroplets and its inhibition by host–guest complexation, *J. Am. Chem. Soc.*, 2022, **144**, 3510–3516.

43 L. Zhao, X. Song, C. Gong, D. Zhang, R. Wang, R. N. Zare and X. Zhang, Sprayed water microdroplets containing dissolved pyridine spontaneously generate pyridyl anions, *Proc. Natl. Acad. Sci. U. S. A.*, 2022, **119**, e2200991119.

44 X. Yuan, D. Zhang, C. Liang and X. Zhang, Spontaneous reduction of transition metal ions by one electron in water microdroplets and the atmospheric implications, *J. Am. Chem. Soc.*, 2023, **145**, 2800–2805.

45 H. Chen, R. Wang, J. Xu, X. Yuan, D. Zhang, Z. Zhu, M. Marshall, K. Bowen and X. Zhang, Spontaneous reduction by one electron on water microdroplets facilitates direct carboxylation with CO_2, *J. Am. Chem. Soc.*, 2023, **145**, 2647–2652.

46 C. Han, C. Li, J. A. Yuwono, Z. Liu, K. Sun, K. Wang, G. He, J. Huang, P. V. Kumar, J. Vongsvivut, J. Cong, H. Mehrvarz, Z. Han, X. Lu, J. Pan, X. Hao and R. Amal, Nanostructured hybrid catalysts empower the artificial leaf for solar-driven ammonia production from nitrate, *Energy Environ. Sci.*, 2024, **17**, 5653–5665.

47 B. Yang, J. Zhao, Y. Xiong, C. Li, M. Zhang, R. D. Rodriguez and X. Jia, Vacancies engineering in ultrathin porous g-C_3N_4 tubes for enhanced photocatalytic PMS activation for imidacloprid degradation, *Chem. Eng. J.*, 2024, **498**, 155117.

48 Z. Wang, G. Ding, H. Huang, J. Zhang, Q. Lv, L. Shuai, Y. Ni and G. Liao, Unraveling the dipole field in ultrathin, porous, and defective carbon nitride nanosheets for record-high

© 2026 The Author(s). Co-published by the Institute of Process Engineering, Chinese Academy of Sciences and Royal Society of Chemistry

Open Access Article. Published on 09 April 2026. Downloaded on 4/9/2026 9:59:55 PM.
This article is licensed under a Creative Commons Attribution-NonCommercial 3.0 Unported Licence.

piezo-photocatalytic H_2O_2 production, *eScience*, 2025, **5**, 100370.

49 B. Dai, J. Guo, C. Gao, H. Yin, Y. Xie and Z. Lin, Recent advances in efficient photocatalysis via modulation of electric and magnetic fields and reactive phase control, *Adv. Mater.*, 2023, **35**, 2210914.

50 Y. Bai, P. Luan, Y. Bai, R. N. Zare and J. Ge, Enzyme-photo-coupled catalysis in gas-sprayed microdroplets, *Chem. Sci.*, 2022, **13**, 8341–8348.

51 K. Li, Q. Ge, Y. Liu, L. Wang, K. Gong, J. Liu, L. Xie, W. Wang, X. Ruan and L. Zhang, Highly efficient photocatalytic H_2O_2 production in microdroplets: Accelerated charge separation and transfer at interfaces, *Energy Environ. Sci.*, 2023, **16**, 1135–1145.

52 Q. Ge, Y. Liu, K. Li, L. Xie, X. Ruan, W. Wang, L. Wang, T. Wang, W. You and L. Zhang, Significant acceleration of photocatalytic CO_2 reduction at the gas-liquid interface of microdroplets, *Angew. Chem., Int. Ed.*, 2023, **62**, e202304189.

53 X. Song, C. Basheer, Y. Xia and R. N. Zare, Oxidation of ammonia in water microdroplets produces nitrate and molecular hydrogen, *Environ. Sci. Technol.*, 2024, **58**, 16196–16203.

54 X. Song, C. Basheer, Y. Xia, J. Li, I. Abdulazeez, A. A. Al-Saadi, M. Mofidfar, M. A. Suliman and R. N. Zare, One-step formation of urea from carbon dioxide and nitrogen using water microdroplets, *J. Am. Chem. Soc.*, 2023, **145**, 25910–25916.

55 Y. Chen, L. Zhang, S. Chen, S. Sun, H. Cheng, S. Li, J. Yu, B. Ding and J. Yan, Synthesis of heteromorphic Bi_2WO_6 films with an interpenetrate 1D/2D network structure for efficient and stable photocatalytic degradation of VOCs, *Adv. Mater.*, 2024, **36**, 2407400.

56 X. Zheng, Y.-G. Fang, M. Tan, B. Chen, J. S. Francisco, C. Zhu and C. Chu, Accelerated methane photo-oxidation at the air - water interface, *J. Am. Chem. Soc.*, 2025, **147**, 26635–26642.

57 J. Li, J. Xu, Q. Song, X. Zhang, Y. Xia and R. N. Zare, Methane C(sp^3)–H bond activation by water microbubbles, *Chem. Sci.*, 2024, **15**, 17026–17031.

58 Y. Wang, H. Shi, Y. Sun, X. Zhang, Y. Li and H. Yang, Locating organocatalysts at pickering droplet interfaces enables promotion of their catalytic enantioselectivity, *J. Am. Chem. Soc.*, 2025, **147**, 31049–31059.

59 D. Yu, F. Zhang, S. Gao, L. Wang, C. Zhang, X. Chen, X. Zhang, S. Chen, X. Fan, X. Yu and Z. Zhao, La-modified manganese-based oxides with amorphous structure: Facile synthesis and mechanistic study for boosting catalytic soot combustion, *Appl. Catal., B*, 2025, **377**, 125516.

60 T. Suguro, F. Kishimoto, N. Kariya, T. Fukui, M. Nakabayashi, N. Shibata, T. Takata, K. Domen and K. Takanabe, A hygroscopic nano-membrane coating achieves efficient vapor-fed photocatalytic water splitting, *Nat. Commun.*, 2022, **13**, 5698.

61 J.-D. Qu, Y. Wang, T.-T. Sun, X.-Y. Chu, Y.-X. Jiang, N.-N. Zhang, Z.-H. Zhao, H. Dong, Y.-Q. Lan and F.-M. Zhang, Engineering covalent organic frameworks for photocatalytic overall water vapor splitting, *Angew. Chem.*, 2025, **64**, e202502821.

62 Y. Wang, W. Huang, S. Guo, X. Xin, Y. Zhang, P. Guo, S. Tang and X. Li, Sulfur-deficient $ZnIn_2S_4$/oxygen-deficient WO_3 hybrids with carbon layer bridges as a novel photothermal/photocatalytic integrated system for Z-scheme overall water splitting, *Adv. Energy Mater.*, 2021, **11**, 2102452.

63 Y. Xu, S. Ai, T. Wu, C. Zhou, Q. Huang, B. Li, D. Tian and X.-H. Bu, Bioinspired photo-thermal catalytic system using covalent organic framework-based aerogel for synchronous seawater desalination and H_2O_2 production, *Angew. Chem.*, 2025, **64**, e202421990.

64 P. Duan, C. Wang, Y. Huang, C. Fu, X. Lu, Y. Zhang, Y. Yao, L. Chen, Q.-C. He, L. Qian and T. Yang, Moisture-based green energy harvesting over 600 hours via photocatalysis-enhanced hydrovoltaic effect, *Nat. Commun.*, 2025, **16**, 239.

65 X. Xin, Y. Zhang, R. Wang, Y. Wang, P. Guo and X. Li, Hydrovoltaic effect-enhanced photocatalysis by polyacrylic acid/cobaltous oxide–nitrogen doped carbon system for efficient photocatalytic water splitting, *Nat. Commun.*, 2023, **14**, 1759.

66 X. Xiong, Z. Wang, Y. Zhang, Z. Li, R. Shi and T. Zhang, Wettability controlled photocatalytic reactive oxygen generation and Klebsiella pneumoniae inactivation over triphase systems, *Appl. Catal., B*, 2020, **264**, 118518.

67 Y. Tang, Z. Qin, Y. Zhong, S. Yin, S. Liang and H. Sun, Three-phase interface photocatalysis for the enhanced degradation and antibacterial property, *J. Colloid Interface Sci.*, 2022, **612**, 194–202.

68 H. Huang, R. Shi, Z. Li, J. Zhao, C. Su and T. Zhang, Triphase photocatalytic CO_2 reduction over silver-decorated titanium oxide at a gas–water boundary, *Angew. Chem., Int. Ed.*, 2022, **61**, e202200802.

69 A. Li, Q. Cao, G. Zhou, B. V. K. J. Schmidt, W. Zhu, X. Yuan, H. Huo, J. Gong and M. Antonietti, Three-phase photocatalysis for the enhanced selectivity and activity of CO_2 reduction on a hydrophobic surface, *Angew. Chem., Int. Ed.*, 2019, **58**, 14549–14555.

70 J.-R. Huang, W.-X. Shi, S.-Y. Xu, H. Luo, J. Zhang, T.-B. Lu and Z.-M. Zhang, Water-mediated selectivity control of CH_3OH versus CO/CH_4 in CO_2 photoreduction on single-atom implanted nanotube arrays, *Adv. Mater.*, 2024, **36**, 2306906.

71 Y. Zhang, CO_2 conversion in water microdroplets, *Adv. Synth. Catal.*, 2025, **367**, e70008.

72 J. Lin, J. He, Q. Huang, Y. Luo, Y. Zhang, W. Li, G. Zhou, J. Hu, Z. Yang and Y. Zhou, Interfacial Bi-O-C bonds and rich oxygen vacancies synergistically endow carbon quantum dot/Bi_2MoO_6 with prominent photocatalytic CO_2 reduction into CO, *Appl. Catal., B*, 2025, **362**, 124747.

73 Y. Ren, Y. Fu, N. Li, C. You, J. Huang, K. Huang, Z. Sun, J. Zhou, Y. Si, Y. Zhu, W. Chen, L. Duan and M. Liu, Concentrated solar CO_2 reduction in H_2O vapour with >1% energy conversion efficiency, *Nat. Commun.*, 2024, **15**, 4675.

74 N. Li, B. Wang, Y. Si, F. Xue, J. Zhou, Y. Lu and M. Liu, Toward high-value hydrocarbon generation by photocatalytic

© 2026 The Author(s). Co-published by the Institute of Process Engineering, Chinese Academy of Sciences and Royal Society of Chemistry

Open Access Article. Published on 09 April 2026. Downloaded on 4/9/2026 9:59:55 PM.
This article is licensed under a Creative Commons Attribution-NonCommercial 3.0 Unported Licence.

reduction of CO_2 in water vapor, *ACS Catal.*, 2019, **9**, 5590–5602.

75 R. Wang, M. Zhang, S. Zhang, J. Zheng, Y. Zeng, Y. Yang, J. Ding, X. Wu and Q. Zhong, Self-supporting triphase photocatalytic CO_2 reduction to CH_3OH on controllable core–shell structure with tunable interfacial wettability, *ACS Nano*, 2023, **17**, 24363–24373.

76 D. Liu, L. Jiang, D. Chen, Z. Hao, B. Deng, Y. Sun, X. Liu, B. Jia, L. Chen and H. Liu, Twin S-scheme g-C_3N_4/$CuFe_2O_4$/$ZnIn_2S_4$ heterojunction with a self-supporting three-phase system for photocatalytic CO_2 reduction: Mechanism insight and DFT calculations, *ACS Catal.*, 2024, **14**, 5326–5343.

77 D. Yao, Z. Chen, C. Chu, X. Ran, X. Liu and S. Mao, Positionally isomeric conjugated polymers for photosynthesis of hydrogen peroxide through triphase interface reaction, *Appl. Catal., B*, 2025, **367**, 125071.

78 R. He, D. Xu and X. Li, Floatable S-scheme photocatalyst for H_2O_2 production and organic synthesis, *J. Mater. Sci. Technol.*, 2023, **138**, 256–258.

79 B. He, C. Luo, Z. Wang, L. Zhang and J. Yu, Synergistic enhancement of solar H_2O_2 and HCOOH production over TiO_2 by dual co-catalyst loading in a tri-phase system, *Appl. Catal., B*, 2023, **323**, 122200.

80 Y. Li, J. Liu, Z. Sun, R. Li, L. Guo, X. Zhang, Y. Wang, Y. Wang, Z. Yu and C. Fan, Enhanced photocatalytic ammonia synthesis over a Bi/carbon cloth float: Triphase reaction system-assisted N_2 supply and photothermal co-activation, *Green Chem.*, 2022, **24**, 9253–9262.

81 J. Liu, R. Li, X. Zu, X. Zhang, Y. Wang, Y. Wang and C. Fan, Photocatalytic conversion of nitrogen to ammonia with water on triphase interfaces of hydrophilic-hydrophobic composite $Bi_4O_5Br_2$/ZIF-8, *Chem. Eng. J.*, 2019, **371**, 796–803.

82 H.-Y. Yang, Y. Zhao, K.-L. Huang and X.-C. Meng, Photothermally catalytic fixation of N_2 over TiO_2 loaded onto carbon paper by fast Joule heating, *Rare Met.*, 2025, **44**, 3206–3217.

83 S. Liu, M. Wang, H. Ji, L. Zhang, J. Ni, N. Li, T. Qian, C. Yan and J. Lu, Solvent-in-gas system for promoted photocatalytic ammonia synthesis on porous framework materials, *Adv. Mater.*, 2023, **35**, 2211730.

© 2026 The Author(s). Co-published by the Institute of Process Engineering, Chinese Academy of Sciences and Royal Society of Chemistry